

Copyright 1972. All rights reserved

PERTURBATION OF NUCLEAR DECAY RATES 5525

G. T. EMERY¹

*Physics Department
Indiana University, Bloomington, Indiana*

CONTENTS

1. INTRODUCTION.....	165
2. DECAY MODES DIRECTLY INVOLVING BOUND ELECTRONS....	167
2.1 ELECTRON CAPTURE.....	167
2.2 INTERNAL CONVERSION.....	169
2.3 MATRIX-ELEMENT EFFECTS AND KINEMATIC EFFECTS.....	175
3. CASES STUDIED.....	175
3.1 ⁷ Be (EC, Δλ, ESCA).....	176
3.2 ⁵⁷ Fe [IC, Δλ, Δ(N/M), ME].....	178
3.3 ⁸⁹ Zr (EC, Δλ); ⁸⁵ Sr (EC, Δλ).....	180
3.4 ⁹⁰ Nb (IC, Δλ).....	181
3.5 ⁹⁹ Tc (IC, Δλ).....	182
3.6 ¹¹⁹ Sn [IC, Δ(O/N), ME].....	183
3.7 ¹²⁵ Te [IC, Δλ, Δ(O/N), ME].....	184
3.8 ¹⁶⁹ Tm [IC, Δ(P/O), ME].....	185
3.9 ¹⁹⁸ Pt (IC, Δλ).....	186
3.10 ²³⁸ U (IC, Δλ).....	186
3.11 OTHER CASES.....	187
4. MACROSCOPIC WAYS OF CHANGING THE RATES OF ELECTRON CAPTURE AND INTERNAL CONVERSION.....	189
4.1 CHEMICAL STATE.....	189
4.2 PRESSURE.....	191
4.3 SUPERCONDUCTIVITY.....	191
4.4 INTERNAL ELECTRIC AND MAGNETIC FIELDS.....	192
4.5 TEMPERATURE.....	193
4.6 PLASMAS.....	193
5. SPECULATIONS AND POSSIBILITIES.....	194
5.1 ALPHA DECAY, BETA DECAY, AND FISSION.....	194
5.2 GAMMA-RAY EMISSION AND HIGHER-ORDER PROCESSES.....	195
5.3 OTHER POSSIBILITIES.....	196

1. INTRODUCTION

One of the paradigms of nuclear science since the very early days of its study has been the general understanding that the half-life, or decay constant, of a radioactive substance is independent of extranuclear considerations. Early

¹ Supported in part by the National Science Foundation.

workers tried to change the decay constants of various members of the natural radioactive series by varying the temperature between 24°K and 1280°K, by applying pressure of up to 2000 atm, by taking sources down into mines and up to the Jungfrauoch, by applying magnetic fields of up to 83,000 Gauss, by whirling sources in centrifuges, and by many other ingenious techniques. Occasional positive results were usually understood, in time, as the result of changes in the counting geometry, or of the loss of volatile members of the natural decay chains. This work was reviewed by Meyer & Schweidler (1), Kohlrausch (2), and Bothe (3). Especially interesting for its precision is the experiment of Curie & Kamerlingh Onnes (4), who reported that lowering the temperature of a radium preparation to the boiling point of liquid hydrogen changed its activity, and thus its decay constant, by less than about 0.05%. Especially dramatic was an experiment of Rutherford & Petavel (5), who put a sample of radium emanation inside a steel-encased cordite bomb. Even though temperatures of 2500°C and pressures of 1000 atm were estimated to have occurred during the explosion, no discontinuity in the activity of the sample was observed.

While the constancy of nuclear decay rates was thus firmly established, the confirming evidence was from studies of alpha- and beta-emitting species. It was pointed out in 1947 by Segrè (6) and by Daudel (7) that in the case of electron-capture decays the decay rate is directly related to the density of atomic electrons at the nucleus, and that, at least for low-*Z* nuclei such as ⁷Be, the effects of different chemical environments should be measurable. The possible effects and some preliminary experimental attempts were discussed by Bouchez et al (8–10). Firm results establishing the effect were obtained by Segrè, Wiegand, and Leininger (11, 12), and were confirmed and extended by Kraushaar, Wilson & Bainbridge (13), and by Bouchez et al (14). The confirmed effects were of the order of 0.1%.

Meanwhile the other radioactive decay process in which atomic electrons participate directly had also been studied. The 6-hr isomer ^{99m}Tc decays principally by internal conversion of a 2.2-keV *E3* transition. Differences in the decay rate for sources in different chemical forms were established by Bainbridge, Goldhaber & Wilson (15, 16) and the chemical and solid-state implications of the results were discussed by Slater (17). The observed effects were of the order of 0.3%.

The revival of interest in this field in recent years may be exemplified by (a) the discovery of chemically induced half-life changes of as large as 3.5% (18), (b) studies of changes in outer-electron internal conversion spectra (19), and (c) a growing awareness of relations between perturbations in nuclear decay rates and the phenomena studied with Mössbauer and ESCA (Electron Spectroscopy for Chemical Analysis) techniques. Parts of the current subject have been discussed, in wider contexts, in earlier reviews by DeBenedetti, Barros & Hoy (20), and by Hollander & Shirley (21). Brief, but more specific, reviews have been given by Daudel (22), Perlman (23), and Perlman & Emery (24).

2. DECAY MODES DIRECTLY INVOLVING BOUND ELECTRONS

2.1 ELECTRON CAPTURE

The weak interaction involved in electron capture and other forms of beta decay is of very short range. This means that the rate of electron capture is essentially proportional to the density at the nucleus of electrons available for capture. The most direct way to change the electron-capture rate is thus to change the total electron density at the nucleus. Extensive accounts of the electron-capture process and its relation to the other modes of beta decay may be found in the treatises of Konopinski (25), Schopper (26), and Wu & Moszkowski (27). Bouchez & Depommier (28) reviewed the subject of electron capture, and more recent results may be found in the *Proceedings* of the Debrecen meeting (29) and in a review by Berényi (30). We follow here the notation used in the tabulation of Behrens & Jänecke (31), which is based on the formulation developed by Bühring, Stech, and Schülke (32-35). [The recent revisions in this formulation (36) are not important for the present discussion.]

The total transition probability for electron capture of orbital electrons is given by

$$\lambda = (g^2/2\pi^2) \sum_x n_x C_x f_x \quad 1.$$

where g is the weak interaction coupling constant, the running index x refers to the various bound atomic orbitals, n_x is the occupation probability of orbital x ($n_x = 1$ when the orbital is full), C_x , to be discussed more fully below, is the capture analog of a beta-spectrum shape factor, and f_x is equivalent to a beta-decay Fermi function. It is given by

$$f_x = (\pi/2) q_x^2 \beta_x^2 B_x \quad 2.$$

The quantity q_x is the energy of the neutrino emitted when an electron hole is left in orbital x . β_x is the wavefunction amplitude for an electron in orbital x ; for s -states ($\kappa = -1$), $\beta_{-1} = g_{-1}(0)$, and for $p_{1/2}$ -states, ($\kappa = +1$), $\beta_{+1} = f_{+1}(0)$. B_x is the exchange and overlap factor of Bahcall (37-41), which takes into account the lack of one-to-one correspondence between processes in which an electron is captured from orbital x in the initial Z atom and those in which a vacancy is left in orbital x of the final $(Z-1)$ atom.

The Coulomb field near a nucleus is very strong. The shape of electron wavefunctions near the nucleus is thus independent of external perturbations; such perturbations only affect the normalization of the wavefunction in the nuclear region. The most direct effect of chemical or thermodynamic perturbations is then on the product $n_x \beta_x^2$, which measures the density of electrons in orbital x at the nucleus. The factors C_x , given explicitly by Behrens & Jänecke

(31), are combinations of nuclear matrix elements, weighted by factors depending on the shapes of the wavefunctions of electrons bound in the x -orbit. They may be expressed as squares of terms which are power series in αZ and in the nuclear radius, R . For allowed transitions, for example, the leading terms are just the Fermi and Gamow-Teller matrix elements. The correction terms, in all cases while depending on the charge and size of the nucleus, and weakly on its charge distribution (36), and on the momentum transfer, are independent of changes in the wavefunction normalizations in the inner region. The relative contribution of occupied orbits with different angular momentum quantum numbers do depend, in general, on the nuclear matrix elements. For almost all transitions however, the decay is dominated by capture from $s_{1/2}(\kappa = -1)$ and $p_{1/2}(\kappa = +1)$ orbits, and the rates are proportional to $n_{-1}\beta_{-1}^2$ and $n_{+1}\beta_{+1}^2$ respectively.

Exchange and overlap effects can be very important in electron capture. They were first considered by Benoist-Gueutal (42) and by Odier & Daude (43). The application of closure methods by Bahcall (37-41) allowed definite predictions of the factors B_x in Equation 2. Since B_{1s} is always less than one while for the higher shells B_{ns} , $n \geq 2$, is greater than one, such ratios as capture leading to L holes relative to capture leading to K holes are altered. The dominant factor in these alterations is the exchange effect, in which, for example, an electron in the K -shell of the initial atom is captured, but the hole appears in the L_1 shell of the final atom. The effects decrease with increasing Z . The predictions of Bahcall for L/K ratios are confirmed, in general, by experiment (29, 30, 41, 44). The accuracy of experimental M/L capture ratios is not yet sufficient to allow a conclusive test of calculated correction factors (45).

In a rather large percentage of electron captures it may be expected that an electron bound in the initial atom may find itself promoted to the continuum after the capture. This is mostly a shakeoff process due to the sudden change in nuclear charge. In a paper reporting a measurement of the K -electron shakeoff probability in the K -capture of ^{131}Cs , Lark & Perlman reviewed previous experimental and theoretical work (46). Further calculations are reported by Carlson et al (47). The probability of shaking off a K -electron decreases as Z^{-2} , and the probability of shaking off outer electrons can be expected to be somewhat smaller for electron capture than for ordinary (positive or negative) beta-ray emission.

In spite of the dramatic effects on capture ratios in light elements (for example the L/K ratio in ^{37}Ar capture is increased by about 22% by exchange) the effect on total capture rates are much smaller. Bahcall has discussed the situation in some detail (38), and concludes that the fractional change in total capture rate due to exchange and overlap effects is of the order of the average atomic excitation energy divided by the neutrino energy. Aside from cases where the Q -value is not much larger than the K -shell binding energy, the effects are then always small, since the average atomic excitation energy can be estimated to be of the order of a few hundred electron volts (38, 47, 48). Bahcall's estimate of the total change in the decay rate of ^7Be due to overlap and exchange was less than 0.1%

The B -factors are essentially redistribution factors, whose weighted value is approximately one

$$\sum_x n_x \beta_x^2 B_x \approx \sum_x n_x \beta_x^2 \quad 3.$$

The total capture rate is then approximately equal to the sum of Equation 1 with the B -factors left out; with the further approximation that the shape factor, C , has a constant value for capture from $s_{1/2}$ and $p_{1/2}$ orbitals, and is zero otherwise, the total capture rate becomes

$$\lambda = (g/\pi)^2 C \sum_x q_x^2 n_x \beta_x^2, \quad x = s_{1/2}, p_{1/2} \quad 4.$$

This equation is necessarily an approximation: the problem is really a many-body problem, and while the golden-rule matrix elements are dominantly proportional to the initial electron density at the nucleus, both exchange and the effect of atomic excitation on the density of final states do have an effect, even on the total decay rate. The situation is somewhat similar to that in electron shakeoff in beta-ray emission: the total shakeoff probability is given to a high degree of accuracy by calculations in the sudden approximation (47, 49, 50), but the shape of the spectrum is sensitive to the Pauli principle and the details of the two-electron final-state phase space (51, 52).

Until now, in published studies of chemical and other macroscopic perturbations of electron-capture decay rates, the effects of overlap, exchange, and shakeoff have not been considered. The size of these effects on total decay rates will, as we have seen, usually be small, of the order of a part per thousand. But since typical chemical effects are also of the order of a part per thousand, a more careful study of the validity of Equation 4 in the context of chemically induced changes in the quantities n_x and β_x would perhaps be worthwhile.

In situations where there is an appreciable density of free electrons, the rate of electron-capture decay may be affected, or even dominated, by the capture of these continuum electrons. Rates for capture of continuum electrons were first estimated by Bethe & Bacher (53). Detailed discussions, using the modern formulation of the weak interaction and including applications to stellar interiors, have been given by Bahcall (54) (see also Sec. 4.6).

2.2 INTERNAL CONVERSION

A nucleus in an excited state can decay to a lower level by photon emission, or, alternatively, by internal conversion. (Exotic decay modes, such as internal pair formation, two-photon emission, double internal conversion, etc., are not yet relevant in a discussion of rate perturbations, and will not be discussed here.) The total transition probability for decay is a sum of the transition probabilities for the various modes, thus, for the electromagnetic transition from level a to level b

$$\Lambda(a \rightarrow b) = \Lambda_\gamma(a \rightarrow b) + \Lambda_{IC}(a \rightarrow b) \quad 5.$$

The internal conversion process can involve any of the atomic electrons, so

$$\Lambda_{IC}(a \rightarrow b) = \sum_{x'} \Lambda_{IC}(x', a \rightarrow b) \quad 6.$$

where the occupied atomic orbits are described by x' , which is an abbreviation for a principal quantum number n' and a relativistic angular quantum number κ' . The internal conversion coefficient for occupied orbital x' is defined as the ratio of the conversion rate to the gamma-ray rate:

$$\epsilon_{x'}(a \rightarrow b) = \Lambda_{IC}(x', a \rightarrow b) / \Lambda_{\gamma}(a \rightarrow b) \quad 7.$$

The total conversion coefficient is just the sum over occupied orbits of the partial coefficients

$$\epsilon_{Tot}(a \rightarrow b) = \sum_{x'} \epsilon_{x'}(a \rightarrow b) \quad 8.$$

and the total rate for the electromagnetic transition, $a \rightarrow b$, is

$$\Lambda_{Tot}(a \rightarrow b) = \Lambda_{\gamma}(a \rightarrow b) [1 + \epsilon_{Tot}(a \rightarrow b)] \quad 9.$$

Internal conversion is to gamma-ray emission as hyperfine structure is to the observation of nuclear moments in an external field. Internal conversion is an off-diagonal form of hyperfine structure. Most internal conversion is "normal," that is, the internal conversion rates and the rate of gamma-ray emission are proportional to the square of the same nuclear matrix element. Just as in diagonal hyperfine structure (55), this is not necessarily the case when there are appreciable contributions from parts of the electron wavefunctions which lie inside the nuclear charge distribution. Such "penetration" effects have been reviewed by Church & Weneser (56), and their relevance to the present context is discussed briefly in Sec. 5. For cases of normal conversion the coefficients are independent of the details of the structure of the initial and final nuclear states, depending only on the energy and multipole nature of the nuclear transition, and on the atomic wavefunctions. The coefficient for conversion in the x' state of a transition between two nuclear states whose energy differs by k , of multipolarity σL , σ either M or E , is (57, 58)

$$\epsilon_{x'}(\sigma L, k) = \frac{\pi k (e^2 / \hbar c)}{L(L+1)(2L+1)} \sum_{\kappa} B_{\kappa x'}(\sigma L) |R_{x, x'}(\sigma L, k)|^2 \quad 10.$$

where κ describes the angular state of the continuum electron, the coefficients $B_{\kappa x'}(\sigma L)$ are those given by Rose (57),² and the R 's are radial integrals. If the binding energy of the x' orbit is $b_{x'}$ the radial integrals are

² An error in one value of B in this reference is corrected in Ref. 58, footnote 39.

$$R_{\kappa, \kappa'}(ML, k) = \int_0^\infty r^2 dr [g_\kappa(k - b_{\kappa'}, r) f_{\kappa'}(r) + f_\kappa(k - b_{\kappa'}, r) g_{\kappa'}(r)] h_L^{(1)}(kr) \quad 11.$$

$$R_{\kappa, \kappa'}(EL, k) = \int_0^\infty r^2 dr \left\{ [g_\kappa(r) f_{\kappa'}(r) - f_\kappa(r) g_{\kappa'}(r)] k - [f_\kappa(r) f_{\kappa'}(r) + g_\kappa(r) g_{\kappa'}(r)] \frac{d}{dr} \right\} r h_L^{(1)}(kr) \quad 12.$$

where $h_L^{(1)}(kr)$ is a spherical Hankel function of the first kind, g_κ and f_κ are the Dirac radial wavefunctions for outgoing electrons of kinetic energy $k - b_{\kappa'}$, and $g_{\kappa'}$, $f_{\kappa'}$ are the Dirac radial wavefunctions for the initial occupied bound orbit. The B -coefficients tabulated are for fully occupied bound orbits, where the number of electrons is $2|\kappa'|$. If the bound orbit is not fully occupied, they should be multiplied by the occupation probability. The continuum wavefunctions are normalized per unit energy interval, and those Dirac radial components which are large near the nucleus, $g_{-|\kappa'|}$ and $f_{+|\kappa'|}$, are positive there (58).

The theory of internal conversion has been reviewed by Rose (59) and by Listengarten (60), as well as in references previously cited. Detailed accounts of many parts of the subject appear in the proceedings of the Vanderbilt Conference (61). The initial full-scale tabulations of the theoretical coefficients for conversion in the K and L shells were given by Rose (57) and by Sliv & Band (62). More recent, and somewhat technically improved, calculations for the K , L , and M shells have been performed by Hager & Seltzer (63), and by Pauli (64). Results for the N shell, for $Z \geq 60$, have been given by Dragoun, Pauli, & Schmutzler (65). Calculations for several specific nuclear transitions have been performed by Bhalla (66-70). In addition, a computer program for calculating theoretical conversion coefficients has been presented by Pauli (71). All these calculations include the static effects of the finite nuclear size (72, 73). In the tabulations of Rose (57), Sliv & Band (62), and Pauli (64), screening has been treated by the Thomas-Fermi-Dirac method, while Hager & Seltzer (63) and Bhalla used relativistic self-consistent field wavefunctions for the electrons. For the wavefunctions used by Dragoun et al, screening potentials were derived from nonrelativistic SCF calculations. The program of Pauli is adaptable to a variety of treatments of screening.

The most complete calculations for the inner shells are those of Hager & Seltzer (63). As far as one can tell from internal consistency and smoothness, when compared with the other modern results and with the most precise experimental data, these coefficients are accurate to within a few percent. [The set of values given for $Z = 93$, L_2 shell in (63) is in error, however; the preliminary report (74) may be consulted for these coefficients.] The only well-established discrepancy is that L_1 conversion, relative to L_2 and L_3 , of some $E2$ transitions of

about 100 keV energy in the neighborhood of $Z=65$, is found to be larger than is given by the calculations by about 5% (75-77). This discrepancy is made possible by a cancellation in the electron radial integrals (78), and is associated with the smallness of the coefficient itself. Quantum-electrodynamic corrections in the next higher order (79) seem to bring the theoretical results back into agreement with experiment.

Different multipoles have characteristic patterns of conversion, for low energy transitions, in the various subshells of a given major electronic shell. Following the widespread applications of empirically-correlated K/L ratios for multipolarity identification (80), the "fingerprint" patterns for L -shell conversion were identified and used by Mihelich (81) and others (82). The applications of these tools has been reviewed by Graham (83). The patterns are not only characteristic and striking, but they repeat from major shell to major shell. Figure 1 shows the patterns, as given by the calculations, for $Z=72$, $k \approx 0.1$. The patterns change regularly and slowly with atomic number and transition energy, becoming multipolarity-independent in the limit of high energy (84, 85), though there is evidence that the high-energy limit has not yet been reached in heavy atoms at $k \approx 20$ ($E_\gamma \approx 10$ MeV) (86, 87).

It was already pointed out by Slater (17) that the only appreciable contributions to the radial integrals (Equations 11, 12) come from the inner part of the atom. Explicit calculations for particular cases (88, 89) bear this out. For certain types of transitions one may go further. Conversion of magnetic multipole transitions at not too high energies is dominated by conversion in odd-numbered subshells (those with negative κ). This dominance is due to large contributions from "surface" terms (90-92) in the radial integrals. As an example, consider the $s_{1/2}$ to $s_{1/2}$ conversion of $M1$ transitions at low energy; this is the dominant part of $M1$ conversion. From the Dirac equations for the radial amplitudes

$$f_{-1}(r) = \frac{1}{1 + W - V(r)} \frac{d}{dr} g_{-1}(r) \quad 13.$$

where W is the total relativistic energy of the electron, and V is its potential energy. For bound electrons with small binding energy, and free electrons with small kinetic energy, $1+W \approx 2$. The sum of products of radial amplitudes in the integrand of Equation 11 then becomes:

$$g^c f^b + f^c g^b = (2 - V)^{-1} (d/dr) g^c g^b \quad 14.$$

where we have let b and c identify the bound and continuum amplitudes. Furthermore, for low-energy transitions with r not too large,

$$r^2 h_1^{(1)}(kr) \approx -i/k^2 \quad 15.$$

The $M1$ radial integral in this limit thus becomes

$$R_{-1,-1} = -ik^{-2} \int_0^\infty dr (2 - V)^{-1} (d/dr) (g^c g^b) \quad 16.$$

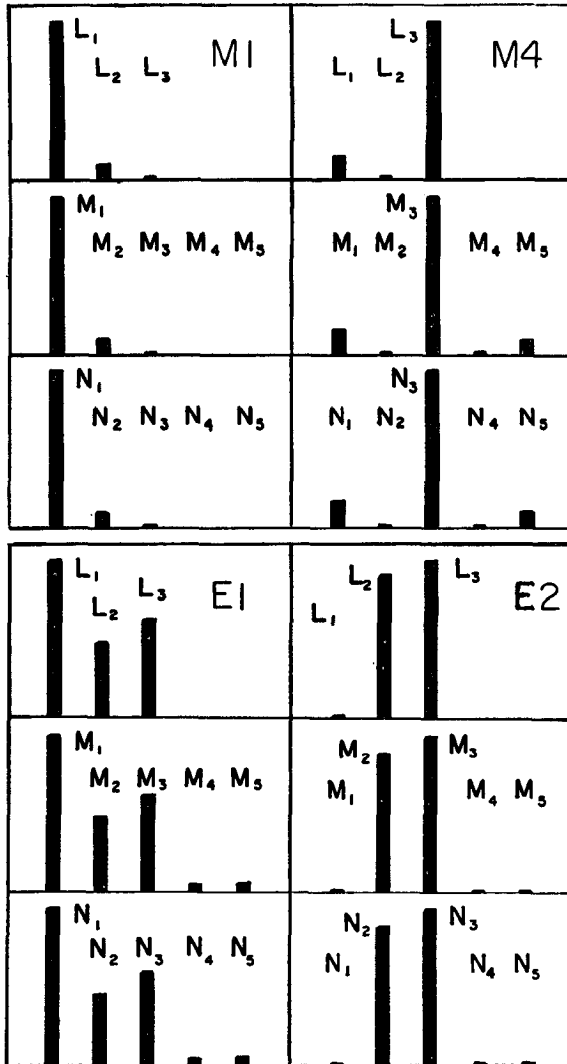


FIGURE 1. Relative conversion coefficients within various atomic shells for different multiplicities. The values shown here are taken from theoretical calculations for $Z=72$ and a transition energy of 51 keV (50 keV for the N -shell). For the L and M shells the results of Hager & Seltzer (63) and Pauli (64), which agree to within a few percent, are used. The N shell results are from Dragoun et al (65). The characteristic "fingerprint" patterns persist throughout the different atomic shells.

and can be integrated by parts

$$R_{-1,-1} = ik^{-2} \int_0^{\infty} dr (g^b g^c) [(d/dr)(2 - V)^{-1}] \quad 17.$$

The factor in the square brackets restricts the effective range of contributions to the integral to a region of the size of Z times the classical electron radius [see the discussion of s -state hyperfine structure by Slichter (93)]. In the nonrelativistic limit, $g(r) = u(r)$, the Schrödinger radial wavefunction, and $f = \frac{1}{2}(du/dr)$, so that

$$R_{-1,-1}(NR) \propto (i/2k^2) u^c(0) u^b(0) \quad 18.$$

which displays even more directly the correspondence between internal conversion and hyperfine structure (94, 95). The remarkable validity of a simple energy dependence for $M1$ conversion in s -states, even up to quite high energies, was noted by Olsson & Hultberg (96); its validity is due to the dominance of the surface terms. The strong correspondence between the relative $M1$ conversion coefficients in various bound s -states and the relative electron-capture intensities has been discussed by Daniel (97). It is also due to the fact that the surface terms are proportional to bound-state electron densities near (which, because of the strength of the Coulomb field, is the same as at) the nucleus. Furthermore, it is through its effects on the normalization of the bound-state wavefunctions that screening is most important. As in the atomic photoeffect (98), the screening effects on the continuum wavefunction normalizations tend to cancel those on the kinematic density of final states.

The surface terms exist, and usually dominate the conversion rates for low energy transitions, for all magnetic multipoles. They occur, in ML conversion, for $\kappa' = -1, \dots, -L$. Such terms do not exist for electric multipole conversion. The dominant radial integrals, however, in both cases, when evaluated directly, have settled to close to their final values by the time the integration has reached a small radius r_{eff} . The explicit calculations by Band et al (89) show that r_{eff} is less than or about equal to $(\ell'+1)(\ell'+2)$ times the K -shell Bohr radius of the atom, where ℓ' is the orbital quantum number of the converting electron. Even for electric multipole conversion, then, that part of the conversion which contributes most to the total rate is proportional to the bound electron densities in the inner part of the atom.

The conclusion is that for the dominant contributions, the relative rates of conversion of the same nuclear transition in two atomic orbitals having the same angular quantum number, κ' , but different radial quantum numbers, n_1' and n_2' , is just

$$\epsilon_{n_1', \kappa'}(\sigma L, k) / \epsilon_{n_2', \kappa'}(\sigma L, k) \approx \left| \psi_{n_1', \kappa'}(0) / \psi_{n_2', \kappa'}(0) \right|^2 \quad 19.$$

This conclusion has been checked experimentally, for example, by Bocquet et al (99), Dragoun et al (100), Pleiter (101), and Fujioka et al (102), and is supported by the calculations, for inner shells, of Church (103) and Pauli (104), and for outer shells, of Dragoun et al (105), and Anderson et al (106). Exchange effects,

and effects of nonperfect overlap of unconverted inner shell wavefunctions, are not expected to be as large in internal conversion as in electron capture. Shake-off of outer-shell electrons may be at least as important as in electron capture. The process was considered by Carlson et al (47), and experimental evidence has recently been presented by Porter et al (107, 108).

2.3 MATRIX-ELEMENT EFFECTS AND KINEMATIC EFFECTS

The rate of a decay process may be written as a product of a matrix-element factor and a factor proportional to the density of final states:

$$\Lambda_{i \rightarrow f} = (2\pi/\hbar) |M_{fi}|^2 \rho(E_f) \quad 20.$$

For the cases of electron capture and internal conversion the states of the final nuclear and bound-atom systems may be considered discrete, and the energy dependence of the density of final states comes almost entirely from the contribution of the outgoing neutrino or electron. Even though there is no unique distinction between the M^2 and the ρ factors, one can make an approximate separation between cases where the rate change is due to changes in the initial bound-state inner-atom electron densities, and where it is due to essentially diagonal shifts in the binding energies. It is mostly the former which will be considered here, since it is through the understanding of the density effects that rate-change studies can make a unique contribution. The diagonal energy shifts are very important in photoelectron spectroscopy (21).

In electron capture the kinematic effects are expressed through the square of the neutrino momentum (Equation 2). Binding energy shifts will change this factor. An example is shown in Figure 2a. Over the region of 10 to 40 keV above the K threshold the fractional change in total electron-capture rate is about 3×10^{-5} per electron volt.

For internal conversion the effects are in general more complicated. When surface terms dominate, however, the conversion rates (in the low-energy limit) are almost independent of binding energy shifts. It then takes the actual crossing of a threshold, or at least coming within a few natural widths of it, to produce an effect. The example of a magnetic dipole transition in lead is shown in Figure 2b. Beyond the threshold, the fractional rate change is about 1×10^{-6} per electron volt. In the neighborhood of the threshold, however, the effects are large. For those internal conversion cases where surface terms do not dominate, conversion just above threshold may have a complicated energy dependence; little is now known about the details.

3. CASES STUDIED

We now review in detail the effects found for ten nuclear transitions, and briefly mention several others. In the subsection headings we use the following abbreviations: *EC*, electron capture; *IC*, internal conversion; $\Delta\lambda$, measured decay rate changes; $\Delta(N/M)$, etc., measured changes in the internal conversion shell ratios; *ME* or *ESCA* indicate that relevant work on the Mössbauer effect

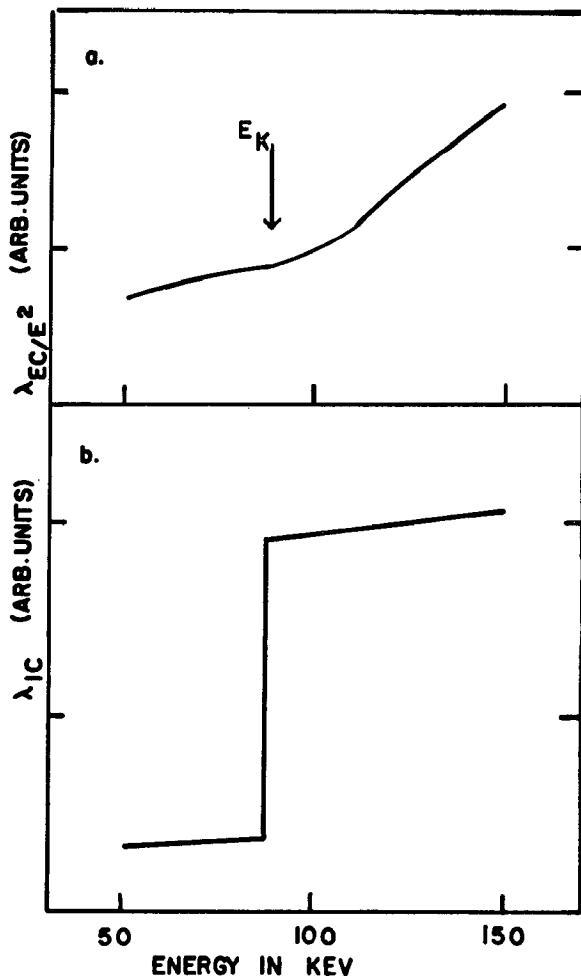


FIGURE 2. Energy dependence of total electron capture and internal conversion rates above and below the *K*-threshold in lead (88.0 keV). (a) Electron-capture rate divided by E^2 , for an allowed transition. (b) Internal conversion rate for an *M1* transition. In both cases the nuclear matrix elements are assumed independent of energy.

or photoelectron spectroscopy have been done. Unless otherwise specified the free-atom electronic configurations are taken from Moore (109).

3.1 ${}^7\text{Be}$ (EC, $\Delta\lambda$, ESCA)

The isotope ${}^7\text{Be}$ decays by electron capture with a half-life of about 53.5 days. About 90% of decays lead to the ${}^7\text{Li}$ ground state; the only radiations are then the very soft Li X-rays, and neutrinos. About 10% of decays lead to an

excited ${}^7\text{Li}$ state, whose decay is signalled by a gamma-ray of 478 keV. Both EC transitions are superallowed, so the shape-function factor (C in Equations 1-4) is state-independent. The nuclear properties are reviewed by Lauritsen & Ajzenberg-Selove (110). The free Be atom has the configuration $(1s)^2(2s)^2$, but screening cuts the ratio of $2s$ to $1s$ electron densities at the nucleus from its hydrogenic value of $1/8$ to approximately 0.04 (111).

In addition to the pioneering work described in Sec. 1, and a further contribution of Bainbridge & Baker (112), the influence of chemical combination on the rate of ${}^7\text{Be}$ decay has now been studied by Johlige, Aumann & Born (113), who have investigated several more compounds. All of the ${}^7\text{Be}$ studies have been done with balanced ionization chambers. The results are summarized in Table 1, which is adapted, in the main, from Johlige et al (113).

One of the confusing aspects of the earlier work concerned discrepancies between the results for BeF_2 , as compared with BeO or Be metal. The Berkeley (11, 12) and Brookhaven (13) results were in good agreement, and gave a change of 0.8×10^{-3} between the metal and the fluoride, but the Paris result (14) was 1.2×10^{-3} . The fluorides were prepared by different methods, and while the Berkeley and Brookhaven samples were shown to be in hexagonal lattice form, the Paris sources were amorphous. The Paris result for amorphous BeF_2 has now been confirmed by Johlige et al. These latter authors point out that the ordering of the different inorganic forms in order of half-life, and therefore electron density at the nucleus, is not the same as the electronegativity ordering.

It is interesting to compare the changes in electron density at the nucleus

TABLE 1. Measured Half-Life Changes Due to Changes in Chemical Combination for ${}^7\text{Be}$

Source pair	Ref.	Result ($\times 10^{-3} \lambda$)
$\lambda(\text{Be}) - \lambda(\text{BeO})$	11	0.15 ± 0.09
	13	0.131 ± 0.05
$\lambda(\text{BeO}) - \lambda(\text{BeF}_2)$	12	0.69 ± 0.03^a
	13	0.609 ± 0.055^a
	113	1.130 ± 0.058^b
$\lambda(\text{Be}) - \lambda(\text{BeF}_2)$	13	0.741 ± 0.047^a
	14	1.2 ± 0.1^b
$\lambda(\text{BeS}) - \lambda(\text{Be})$	112	0.53 ± 0.06
$\lambda(\text{BeO}) - \lambda(\text{BeBr}_2)$	113	1.472 ± 0.063
$\lambda(\text{BeO}) - \lambda(\text{Be}(\text{C}_6\text{H}_6)_2)$	113	0.795 ± 0.074
$\lambda(\text{Be}^{2+}(\text{OH}_2)_4) - \lambda(\text{BeO})$	113	0.374 ± 0.077
$\lambda(\text{Be}_4\text{O}(\text{CH}_3\text{COO})_6) - \lambda(\text{BeO})$	113	0.724 ± 0.057
$\lambda(\text{Be}^{2+}(\text{OH}_2)_4) - \lambda(\text{Be}(\text{C}_6\text{H}_6)_2)$	113	1.169 ± 0.106
$\lambda(\text{Be}_4\text{O}(\text{CH}_3\text{COO})_6) - \lambda(\text{BeF}_2)$	113	1.852 ± 0.082^b

^a BeF_2 in the hexagonal form.

^b BeF_2 in the amorphous form.

with the changes in K electron binding energies observed in ESCA work. ESCA results (114, 115) are available for Be, BeO, and BeF₂ (degree of crystallinity unspecified). While the ordering is the same as for change in half-life (and the K electrons are more tightly bound in BeF₂ than in Be metal) the effects are not proportional; the splitting between metal and oxide is 2.9 ± 0.1 eV, while that between oxide and fluoride is only 1.3 eV.

The change in half-life between the gaseous and the metallic states was estimated by Jacques (116), using a variety of methods; effects of the order of 3.5% were predicted.

3.2 ⁵⁷Fe [IC, $\Delta\lambda$, $\Delta(N/M)$, ME]

States in ⁵⁷Fe are populated in the decay of 270-day ⁵⁷Co. Of particular interest is the decay of the 14.4-keV first excited state of ⁵⁷Fe to the ground state. The 14.4-keV transition, familiar in Mössbauer-effect spectroscopy (20, 117), is predominantly $M1$, with an $E2$ admixture of about $(5 \pm 2) 10^{-6}$. The total conversion coefficient of the transition is about 8.3. The available information about this transition has been compiled by Rapaport (118). The neutral iron atom has the configuration $(3d)^6(4s)^2$ outside the argon closed shells.

Extensive data on the ME isomer shift for compounds of iron is available; these results give the product of change in mean-square charge radius between the ground and 14.4-keV states, times the change in total electron density at the nucleus between the source and absorber chemical forms. The relative change in charge radius, typically of the order of 10^{-3} to 10^{-4} , is not determinable in any other practicable way. After the isomer shift was discovered in ⁵⁷Fe (119), estimates of the changes in electron density at the iron nucleus in various compounds were made by Walker, Wertheim, & Jaccarino (120), who derived a value for $\Delta R/R$ which is (when corrected for relativistic effects) 1.4×10^{-3} . Consideration of "overlap-induced" s -electron density changes led Šimánek and collaborators (121, 122) to revised estimates of $\Delta R/R \approx 0.4$ to 0.5×10^{-3} . All these atomic and chemical arguments lead to the conclusion that the 14.4-keV state charge radius is smaller than that of the ground state.

The method of studying changes in the relative intensity of outer-electron internal conversion lines (19) was applied to ⁵⁷Fe by Pleiter & Kolk (123). Their tabulated data are plotted in Figure 3, which shows the variation in the measured N/M_1 ratio, which is essentially the $4s/3s$ electron density ratio, vs the measured isomer shift. They concluded that $\Delta R/R = (0.45 \pm 0.15) 10^{-3}$. The experimental resolution of Pleiter & Kolk was $(\Delta p/p) \approx 0.2\%$, and thus the N -line was only partly resolved from the M -line.

Results of measurements at higher resolution ($\approx 0.05\%$) were reported by Porter & Freedman (108). They prepared ⁵⁷Co sources with an isotope separator. When ⁵⁷Co ions were deposited on the surface of graphite (and thus in what was labelled an "oxide" state) they found the ratio $N_1/M_1 = 0.024 \pm 0.002$, while when 500-eV ions penetrated into the graphite (labelled a "metallic" state) they observed $N_1/M_1 = 0.034 \pm 0.003$. A disturbing feature was found, however, in

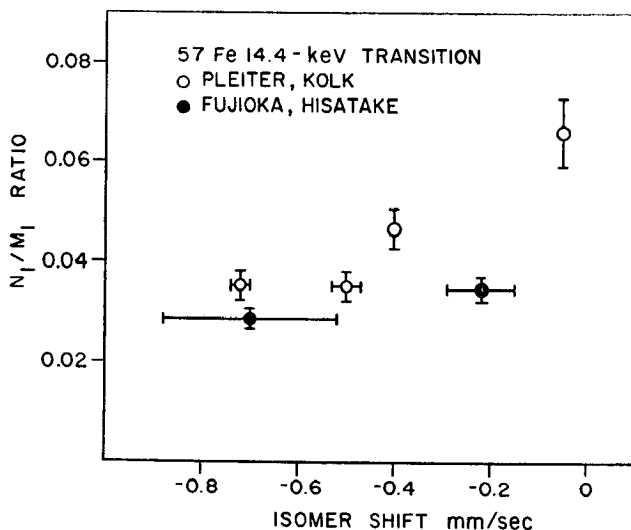


FIGURE 3. Measured N_1/M_1 ratios in internal conversion of the 14.4-keV transition in ^{57}Fe , as a function of the Mössbauer-effect isomer shift of the source relative to $\text{K}_4\text{Fe}(\text{CN})_6 \cdot 3\text{H}_2\text{O}$. N/M ratios of Pleiter & Kolk (123) for different runs with the same source have been averaged. The measured isomer shifts of Fujioka & Hisatake (124) have been adjusted for the SS 310-potassium ferrocyanide difference.

their high-resolution work: the N_1 lines shapes showed less low-energy tail than the M_1 line shapes, and the difference could not be attributed to differences in electron energy loss in the sources. Porter & Freedman concluded that the shape difference was probably due to a difference in the amount of outer-electron shakeoff associated with the conversion. Their concurrent studies of L -shell shakeoff in K -electron conversion (107) suggest support of this view. They also noted that it could be misleading to derive results from data taken at lower resolution, without some knowledge of these line-shape changes. The K -electron binding energy was found to be 3.3 eV higher for the "oxide" source than for the "metallic" source.

Results of further high-resolution measurements have now been reported by Fujioka & Hisatake (124), who compared the conversion spectra (and isomer shift) of ^{57}Co sources deposited on a cobalt metal substrate, with and without annealing. They confirm the line-shape difference (108). Their N_1/M_1 ratios, vs isomer shift, are compared with those of Pleiter & Kolk in Figure 3. Fujioka & Hisatake conclude that $\Delta R/R \gtrsim 0.6 \times 10^{-3}$. See also (272, 273).

Attempts to determine the change in half-life of the 14.4-keV state associated with sources having different isomer shifts are now in progress (125). The usefulness of this technique, which avoids difficulties connected with inner-electron

readjustment to changes in outer-electron wavefunctions or occupation numbers, was discussed by Raff, Alder & Baur (126), who gave specific results for the relation between the two effects, as a function of $\Delta R/R$.³

In iron it is the $3d$ electrons which give the large atomic magnetic moment. The field of the $3d$ electrons is strong enough to polarize, to some extent, the s -states. That the inner s -states were polarized in ferromagnetic iron was already deduced from the magnitude and sign of the magnetic field at the nucleus, as seen in the Mössbauer effect (127, 128). The resulting energy splitting of the s -states was first established by Fadley et al (129), who found a splitting of about 4.4 eV for the $3s$ electrons. The $2s$ and $3s$ electron spin densities in iron have now been studied by Song et al (130), who observed the internal conversion decay of the 14.4-keV level after excitation by polarized Mössbauer gamma-rays. Calculations related to the effects have been performed by Morita and collaborators (131, 132).

3.3 ^{89}Zr (EC, $\Delta\lambda$); ^{85}Sr (EC, $\Delta\lambda$)

The isotope ^{89}Zr has a half-life of 78.4 hrs and decays to levels in ^{89}Y . The spin and parity of ^{89}Zr are $9/2+$, and 99% of the decay (76.6% by EC and 22.3% by positron emission) feeds directly the $9/2+$ state at 909 keV in ^{89}Y ; another 1% of decays are by EC to higher excited states. While the $\log ft$ of the principal EC transition is 6.1, indicating some hindrance, it can be understood as due to relatively low occupation, in ^{89}Zr , of pairs of protons in the $g9/2$ state. The "shape factor," C in Equation 1, should then be independent of atomic orbit. The data on mass 89 nuclei have been quoted from a recent evaluation (133). The atomic ground state of zirconium is $(4d)^2(5s)^2$ outside the krypton closed shell.

Gagneux et al (134) have grown barium titanate crystals with active ^{89}Zr replacing some of the titanium ions. Barium titanate has a ferroelectric phase transition at 120°C; above that temperature it has a perovskite cubic structure, while below it the structure becomes deformed, and there are large internal electric fields. Gagneux et al interchanged pairs of $\text{BaTi} (^{89}\text{Zr})\text{O}_3$ sources viewed by NaI detectors, with provisions for heating one or both of the sources. They used both what they called the "Steigungs" method, in which the change with time of the ratio of the counting rates, was followed, and what they called the " $\Delta\lambda$ -Sprung" method, in which the change in counting rate due to a change in temperature was determined, with the temperature cycled above and below the Curie point on a relatively short time scale. The result was that ^{89}Zr decayed more slowly in ferroelectric BaTiO_3 than in the cubic form. The measured change in the total decay rate was found to be $\Delta\lambda/\lambda = (6.2 \pm 0.2) 10^{-4}$, while for the electron capture part alone, $\Delta\lambda_{\text{EC}}/\lambda_{\text{EC}} = (8.0 \pm 0.3) 10^{-4}$.

As discussed in Sec. 4, the internal electric field by itself probably has little effect on the EC decay rate, and the major part of the change probably comes

³ Results of such an experiment have now been reported by Rügsegger & Kündig (126a), who deduce that $\Delta R/R = (0.31 \pm 0.06) 10^{-3}$.

from the change in electron density at the nucleus due to the displacement of the ^{89}Zr from its symmetrical position in the unit cell.

Preliminary results of similar measurements with ^{85}Sr in BaTiO_3 have been reported (135). The EC decay of ^{85}Sr ($T_{1/2} = 65.2$ days) is similar to that of ^{89}Zr , except that there are no positrons (136). The sign of the effect is the same as for ^{89}Zr , but the magnitude is much smaller (135): $\Delta\lambda/\lambda = (0.49 \pm 0.29) 10^{-4}$. The difference may be related to the fact that, while the Zr atom has the same d^2s^2 configuration as the Ti for which it is substituted, the free Sr atom has no 4d electrons.

3.4 ^{90}Nb (IC, $\Delta\lambda$)

States of ^{90}Nb are populated in the decay of 5.7 hr ^{90}Mo ; the relevant nuclear data are reviewed by Ball, Johns & Way (137). Approximately 90% of ^{90}Mo decays lead to the feeding of a state of spin and parity 4- at 124.8 keV in ^{90}Nb . This state has a half-life of 18.82 ± 0.09 sec (138); earlier measurements had led to values of up to 24 sec. The 18.8-sec isomer decays by a low-energy transition to a 6+ state at 122.4 keV, which in turn decays to the 8+ ground state by an $E2$ transition. The energy of the isomeric transition is reported as 2.38 ± 0.36 keV (139), and its multipolarity is almost certainly $M2$. A low energy $M2$ transition converts principally in $s_{1/2}$ and $p_{3/2}$ atomic orbitals. The atomic ground state of niobium is $(4d)^4(5s)$ outside the krypton closed shell.

Cooper, Hollander & Rasmussen (140) perturbed the decay rate of this isomeric transition by changing the chemical state of the activity and thus producing an immediate change in the intensity of the 122-keV transition, which follows the isomeric transition with a half-life of only $(61 \pm 4) 10^{-6}$ sec (141), relative to transitions following the decay of ^{90}Nb ground state (14.6 hr). The 122-keV intensity relaxes to equilibrium with the half-life of the isomer. Niobium foils were bombarded with 50-MeV protons, and thus ^{90}Mo was produced by the $(p, 4n)$ reaction. The foils were dissolved in a mixture of hot concentrated nitric and hydrofluoric acids; the chemical state was thus changed from metallic to that of a fluoride complex. The result was $\lambda(\text{Nb metal}) - \lambda(\text{fluoride complex}) = (3.6 \pm 0.4) 10^{-2} \lambda(\text{fluoride complex})$.

A somewhat different result was obtained by Weirauch et al (142). These authors prepared the 19-sec isomer directly, with the reaction $(d, 2n)$, by bombarding pairs of zirconium foils with 19-MeV deuterons. The decay rate with the activity in the irradiated Zr foil was within one percent of that when the foil was dissolved in an HNO_3 -HF mixture. The activity was also produced directly by Geiger et al (138), through the reaction $\text{Zr}(p, n)$ with Zr targets and with Hf targets in which Zr was an impurity. The half-lives were the same within about 1.5%.

The experiment of Cooper et al (140) was repeated by Olin (143), who found $\lambda(\text{Nb metal}) - \lambda(\text{fluoride complex}) = (3.9 \pm 0.8) 10^{-2} \lambda(\text{Nb metal})$ in good agreement. Olin also determined that $\lambda(\text{Nb}_2\text{O}_5) - \lambda(\text{Nb metal}) = (1.87 \pm 0.50) 10^{-2} \lambda(\text{Nb metal})$.

The measurement of Weirauch et al was also repeated by Smend, Borchert & Langhoff (144). The new result was that the fractional change in isomeric half-life between ^{90m}Nb in Zr metal and in the fluoride complex was $<0.18 \cdot 10^{-2}$.

It is not easy to interpret all these results in a consistent manner. If the fluoride complexes in (142) and (144) are the same as those in (140) and (143), then the decay rate of ^{90m}Nb in Nb differs from that in Zr by 3–4%. The “metallic” sources themselves have had different radiation and decay histories, and the nature of the sites occupied by the isomeric systems have not been determined.

An influence of superconductivity on the half-life of ^{90m}Nb has been studied by Olin & Bainbridge (145). Sources prepared in a manner similar to those in (143) were held at liquid helium temperature. A 4-kG magnetic field was used to quench the superconductivity. When the field was removed, the recovery of the 122-keV gamma-ray intensity to equilibrium followed. It was found that ^{90m}Nb decays more slowly in the superconducting state than it does when the superconductivity is quenched by a magnetic field: $\lambda(\text{normal}) - \lambda(\text{superconducting}) = (0.195 \pm 0.055) \cdot 10^{-2} \lambda(\text{normal})$. An earlier attempt by Cooper (146), in which the superconducting transition was induced by temperature change and observed by flux expulsion, led to an upper limit of $\sim 0.2 \times 10^{-2}$ for $|\Delta\lambda|/\lambda$.

The effect of high pressure on the decay rate of ^{90m}Nb was investigated by Cooper (146) who found that $\lambda(0.1 \text{ megabar}) - \lambda(0) = (6.3 \pm 7) \cdot 10^{-3} \lambda(0)$.

For further discussion of the chemical and superconducting effects in Nb see Sec. 4. It was pointed out by Olin (143) that the L_3 -electron binding energy in Nb is within experimental uncertainty of the transition energy. If L_3 conversion is fully allowed it should account for about 2/3 of the total decay rate. Then if the L_3 binding energy is slightly below the transition energy in Nb metal, when it increases slightly in the fluoride complex the decay rate will decrease. It would be of great interest to know more precisely the energy of the isomeric transition, the fraction of L_3 conversion, and the chemical and superconducting binding energy shifts in niobium.

3.5 ^{99}Tc (IC, $\Delta\lambda$)

The isomeric activity ^{99m}Tc is a daughter of ^{99}Mo (67 hr) and decays with a half-life of 6.0 hr. The isomer has spin and parity $1/2^-$; about 0.8% of decays go directly to the ^{99}Tc ground state ($9/2^+$) by an $M4$ transition of 142.7 keV. The remaining decays are by a low-energy $E3$ transition to a $7/2^+$ state at 140.5 keV, which decays to the ground state by an $M1$ transition. The nuclear data are summarized in the *Table of Isotopes* (147). The energy of the predominant isomeric transition has been determined to be 2.17 ± 0.01 keV by Lacasse & Hamilton (148), who also studied the conversion ratios: $M_2/M_3/M_{46}/N = (56.4 \pm 2)/100/(47.6 \pm 2)/(28.6 \pm 5)$. These ratios are in close agreement with those found by interpolation in tables of theoretical coefficients (63). The total conversion coefficient is then about 1.4×10^{16} . The atomic ground state of TC is $(4d)^5(5s)^2$.

The first demonstration that the half-life of an isomeric transition could be changed by chemical means was performed with ^{99m}Tc , by Bainbridge, Goldhaber & Wilson (15, 16). The comparison of two compounds in which Tc was

in the +7 valence state showed that $\lambda(\text{KTcO}_4) - \lambda(\text{Tc}_2\text{S}_7) = (2.70 \pm 0.10) 10^{-3} \lambda(\text{Tc}_2\text{S}_7)$. This result is for the pertechnetate in the dry salt; the same value, within the uncertainty, was found for KTcO_4 in basic aqueous solution. Sources with the ^{99m}Tc in Tc metal varied in half-life by $\sim 0.3 \times 10^{-3}$ according to the method of preparation, but reproducible results were obtained with sources prepared by an electroplating procedure followed by reduction (16). With these sources it was found that $\lambda(\text{Tc}) - \lambda(\text{Tc}_2\text{S}_7) = (0.31 \pm 0.12) 10^{-3} \lambda(\text{Tc}_2\text{S}_7)$. A source of partly amorphous Tc, reduced from bulk Tc_2S_7 , decayed more slowly than ^{99m}Tc in unreduced Tc_2S_7 , by about one part in 10^3 .

These results were considered by Slater (17), who pointed out that the major effect is probably due to the squeezing of the 4*p* electrons in KTcO_4 , with its smaller interatomic distances.

The influence of temperature and the superconducting transition on this lifetime were studied by Byers & Stump (149). No difference was found between the decay constant at 77°K and 293°K. At 4.2°K measurements were made without magnetic field, and thus in the superconducting state, and with a field of 5.3 kG (normal state) with the results $\lambda(4.2^\circ\text{K}, \text{superconducting}) - \lambda(293^\circ\text{K}) = (0.64 \pm 0.04) 10^{-3} \lambda(293^\circ\text{K})$, $\lambda(4.2^\circ\text{K}, \text{normal}) - \lambda(293^\circ\text{K}) = (0.13 \pm 0.04) 10^{-3} \lambda(293^\circ\text{K})$. The sign of the superconducting effect is opposite to that found for ^{99m}Nb (145) (see Sec. 4).

Balanced ionization chambers were used in all the above work on ^{99m}Tc . Bainbridge, Goldhaber & Wilson give a detailed discussion of the technique (16).

Effects of compression on the decay rate of ^{99m}Tc in Tc metal were studied by Bainbridge (150), who found that $\lambda(0.1 \text{ megabar}) - \lambda(0) = (0.23 \pm 0.05) 10^{-3} \lambda(0)$, and by Mazaki, Nagatomo & Shimizu (151), who found $\lambda(0.1 \text{ megabar}) - \lambda(0) = (0.46 \pm 0.23) 10^{-3} \lambda(0)$. Effects of just this order of magnitude were calculated for this case by Porter & McMillan (152).

Studies of the influence of an external electric field on the ^{99m}Tc decay rate have been undertaken by Leuenberger et al (153), who have mixed Tc and Tc compounds with a dielectric powder, and put it in a capacitor in fields of $\sim 2 \times 10^4$ V/cm. Decay rate changes of the order of $\Delta\lambda/\lambda \approx 10^{-4}$ have been observed.

Nishi & Shimizu (154) have studied the effects of the ferroelectric phase transition in BaTiO_3 on the half-life of substituted ^{99m}Tc . A differential method was used. The fractional change in decay constant was found to be $(2.6 \pm 0.4) 10^{-3}$, with faster decay in the paraelectric phase.

In their study of the conversion-lines of the 2.17-keV isomeric transition, Lacasse & Hamilton observed satellite peaks, with intensities 10–20% of the main peaks, at energies about 50 eV above the M_2 , M_3 , and M_{45} lines. Several simple explanations could be ruled out. The possibility that the satellite peaks corresponded to part of the source being in a different chemical form was considered, but no conclusion could be reached.

3.6 ^{119}Sn [IC, $\Delta(\text{O/N})$, ME]

The first excited state of ^{119}Sn lies at 23.875 ± 0.010 keV, has $I\pi = 3/2+$, and

decays to the ground state by an $M1$ transition. The transition has been used extensively in Mössbauer-effect studies. Neither $E2$ admixture nor penetration effects in the $M1$ conversion have been observed. Conversion takes place in the L , M , N & O shells; the total conversion coefficient is 5.13 ± 0.15 (155) and the half-life of the 24-keV state is 17.75 ± 0.12 nsec (156). The ground state of the free tin atom is $(4d)^{10}(5s)^2(5p)^2$ outside the krypton closed shell.

Effects of chemical combination on a spectrum of internal conversion electrons were first observed by Bocquet et al (19) in a study of this transition, with ^{119m}Sn (245 day) sources. The chemical forms compared were white tin metal and SnO_2 . To get good electron spectra at this energy, sources must be thin, but measurement of Mössbauer spectra of the same sources confirmed that the radioactive atoms were in the same environment as ^{119m}Sn in bulk metal and dioxide. Momentum resolutions of 0.10 to 0.15% were attained. Contributions from K - LM Auger lines in the same energy region had to be accounted for. It was found that the O/N intensity ratios were 0.108 ± 0.004 for white tin and 0.074 ± 0.004 for SnO_2 . Effects of a possibly different line shape for the N and O lines, as observed for ^{57}Fe by Porter & Freedman (108), were not taken into account; such effects, while probably smaller in the Sn case than in the Fe, due to the higher energy and poorer spectrometer resolution, should lead to an increase in the uncertainties. No changes were seen in the relative conversion intensities of the more tightly bound electrons (99).

Consequences of this chemical effect on $5s$ conversion for the interpretation of the Mössbauer isomer shift were also considered. Estimates based on chemical arguments of the change of electron density at the nucleus in going from one chemical form of Sn to another have led to some disagreement about the magnitude, and even the sign, of $\Delta R/R$ (157–166). The experiment showed directly that the charge radius of the 24-keV state was larger than that of the ground state (19). The final conclusion (167) was that $\Delta R/R = (1.84 \pm 0.37) 10^{-4}$. It was also noted that several previous isomer-shift calibrations not only did not agree with the measured $5s$ conversion intensity change, but in fact did not agree with either of the measured O/N ratios. Another “experimental” calibration, by Rothberg, Guimar & Benczer-Koller (168), based on a comparison of isomer-shift temperature dependence and NMR Knight shift, gives the result $\Delta R/R = (1.8 \pm 0.4) 10^{-4}$.

3.7 ^{125m}Te [IC, $\Delta\lambda$, $\Delta(O/N)$, ME]

^{125m}Te has a half-life of about 58 days, spin and parity $11/2^-$, and decays by an $M4$ transition of 109.4 keV to the first excited state. This state ($3/2^+$, $T_{1/2} = 1.5$ ns) decays to the ground state ($1/2^+$) by a 35.6-keV $M1$ transition. The 35.6-keV transition has been used in Mössbauer studies and has a total conversion coefficient of 13.2; the $E2$ admixture is only $(0.035 \pm 0.020)\%$. Both transitions convert in the K , L , M , N , and O shells. The $M4$ transition converts about twice as strongly in p states as in s states (147, 169–171). The atomic ground state of tellurium is $(4d)^{10}(5s)^2(5p)^4$ outside the krypton closed shell.

Changes in the decay rate of ^{125m}Te in the chemical forms Te metal, Te oxide,

and silver telluride were studied by Malliaris & Bainbridge (172). Balanced ionization chambers were used. The results were

$$\begin{aligned}\lambda(\text{Te}) - \lambda(\text{Ag}_2\text{Te}) &= (2.59 \pm 0.18) 10^{-4} \lambda(\text{Te}), \\ \lambda(\text{TeO}_2) - \lambda(\text{Ag}_2\text{Te}) &= (2.23 \pm 0.18) 10^{-4} \lambda(\text{Te}), \\ \lambda(\text{Te}) - \lambda(\text{TeO}_2) &= (0.36 \pm 0.17) 10^{-4} \lambda(\text{Te})\end{aligned}$$

Martin, Erickson & Perlman (173) have tried to determine the change in *O*-shell conversion of the 35.6-keV transition between sources of Te metal and Ag₂Te. A limit of 5% could be put on *O*-shell change relative to the other lines. Somewhat larger effects were reported by Makariūnas, Kalinauskas & Davidonis (174), who found $O/N(\text{Te})=0.152 \pm 0.017$, $O/N(\text{ZnTe})=0.108 \pm 0.015$, $[O/N(\text{Te})]/[O/N(\text{ZnTe})]=1.41 \pm 0.34$.

Consistent relative calibrations of the isomer shift in the Mössbauer effect for isoelectronic compounds of Te, Sn, and neighboring species have been developed by Ruby & Shenoy (175).

3.8 ¹⁶⁹Tm [IC, Δ(P/O), ME]

¹⁶⁹Tm has a permanent quadrupole deformation. Its ground state and first excited state are the $I=1/2$ and $3/2$ members of an even-parity rotational band with an intrinsic angular momentum component along the symmetry axis of $K=1/2$. The transition between them is at 8.401 ± 0.008 keV, and is predominantly $M1$ with an $E2$ admixture of $0.108 \pm 0.005\%$ (176). Even with such a small admixture, about 40% of the conversion is due to $E2$ conversion in *p* states, with the remainder $M1$ conversion, mostly in *s* states. Conversion takes place in the *M*, *N*, *O*, and *P* shells. If one takes the total *M*-shell coefficient from theory (63), for the admixture given, and multiplies by the experimental ratio $MNOP/M$, one finds that the total conversion coefficient is about 266; experimental values are 325 ± 35 (177) and 220 ± 50 (178). The 8.4-keV state has a half-life of 4.04 ± 0.06 nsec (179). The transition occurs following decay of both ¹⁶⁹Er (9.4 day) and ¹⁶⁹Yb (32 day), and is widely used in Mössbauer studies. The ground state of the free thulium atom is $(4f)^{13}(6s)^2$ (180), while the trivalent ion has $(4f)^{12}$ (181).

Carlson, Erman & Fransson (176) have observed changes in the *P/O*₁ ratio in internal conversion with changes in chemical form. Spectrometer momentum resolutions of $\sim 0.2\%$ were used. Sources of ¹⁶⁹Er in various solids were prepared with an isotope separator. The results are given in Table 2. It was assumed that the *P* and *O* line shapes were the same. Interpretation of the results in terms of electron density at the nucleus is complicated by a possible contribution from *6p* bonding electrons. Equal numbers of *6p* and *6s* electrons should lead to 15–20% of the *P* line intensity coming from *p* electrons, so the major effect is undoubtedly an *s*-electron effect.

Studies of the Mössbauer-effect isomer shift for the 8.4-keV transition lead to the conclusion that the charge radius of the excited state is smaller than that of the ground state (182).

TABLE 2. Relative intensities of the P and O_1 conversion lines of the ^{169}Tm 8.4-keV Transition in different chemical environments^a

Probable chemical environment	P/ O_1
W metal	0.056 ± 0.007
WO_3	0.030 ± 0.006
Tm_2O_3	0.035 ± 0.006
Fe_2O_3	0.03 ± 0.01

^a Carlson, Erman & Fransson (176).

3.9 ^{193}Pt (IC, $\Delta\lambda$)

States in ^{193}Pt are excited in the decay of ^{193}Au (16 hr) and ^{193m}Pt (4.3 day). ^{193}Pt is itself unstable, with an electron capture Q -value of 60.8 ± 3.0 keV and a partial half-life for L -capture of 620 ± 250 yr (183). Several puzzling features of the level scheme of ^{193}Pt were explained by Johansson et al (184, 185), who found that the first excited state was at an energy of only 1.644 ± 0.004 keV. From conversion spectra and the nature of transitions feeding the ground and 1.64-keV states it could be concluded that the transition between them was primarily of $M1$ character. Conversion was observed in the N_1 , N_2 , and O_1 shells, and may be expected in the P shell as well. The half-life of the 1.64-keV state was found to be 9.7 ± 0.3 nsec (186). From the tabulated theoretical N -shell coefficients for an $M1$ transition (65), with a correction for the O and P shells, one estimates that the total conversion coefficient is in the neighborhood of 1.5×10^4 . The ground and first excited states are assigned spin and parity $1/2^-$ and $3/2^-$, respectively (185). Platinum has the free-atom configuration $(5d)^9(6s)$.

Chemical effects on the lifetime of the 1.64-keV state have been studied by Marelius (186). Sources of ^{193}Au were used, in Au metal and AuCl_3 . Half-lives were measured directly by electron-electron delayed coincidence in a double long-lens spectrometer with 20 kV preacceleration. It was found that the half-life was $4 \pm 2\%$ longer in the chloride source than in the metallic source.

3.10 ^{235}U (IC, $\Delta\lambda$)

It was found in 1957 that the first excited state of ^{235}U , which is populated in the alpha decay of ^{239}Pu and has $I\pi = 1/2^+$, has a very low excitation energy and decays to the ground state with a half-life of about 26 min (187, 188). The experimental information on this isomeric decay has recently been reviewed by Artna-Cohen (189), who adopts an average half-life of 26.1 min. The most recent determination of the transition energy is that of Nève de Mévergnies (190), who found 73 ± 5 eV; earlier results had been $\lesssim 23$ eV (191), 75 eV (192), and 30 ± 3 eV (193, 194). The spins and parities of the levels are well known and thus the transition would be expected to be $E3$. The ground-state configuration of the free uranium atom is $(5f)^3(6d)(7s)^2$ outside the radon core (195, 196). If the energy is near 73 eV, conversion is possible only in $6s$, $6p$, $5f$, $6d$, and $7s$ states (197). Conversion of low-energy $E3$ transitions takes place primarily from p

and *d* bound electronic states. In this case then, almost all of the conversion will be from the *6p* states, with perhaps a few percent from the *6d* state.

The effect of chemical state on the half-life of this isomeric decay was studied by Mazaki & Shimizu (198, 199). Recoils from ²³⁹Pu alpha decay were collected on carbon films and silicon crystals, and on platinum. The activity was diffused into the carbon and silicon, and the resulting chemical states were thought to be like UC and USi. The activity on Pt was thought to be a metallic state. Pairs of these sources were mounted alternately as the first dynodes of two electron multipliers, and differential comparisons made. It was found that

$$\begin{aligned}\lambda("U") - \lambda("UC") &= (0.318 \pm 0.050)10^{-2}\lambda("U"), \\ \lambda("U") - \lambda("USi") &= (0.221 \pm 0.036)10^{-2}\lambda("U"), \\ \lambda("USi") - \lambda("UC") &= (0.097 \pm 0.043)10^{-2}\lambda("USi")\end{aligned}$$

Detailed studies of environmental effects on this half-life have been made by Nève de Mévergnies (200–202). Recoil sources were collected, either in vacuum, with the atoms entering the collector with their recoil energy of ≈ 90 keV, or in one atmosphere of argon, with the charged, but slowed down, recoils pulled to the collector with a field of ~ 6 kV/cm. Decay rates were compared with a proportional flow counter with two source positions. Half-life differences were found (201) between sources collected in the two ways, and between the low-energy (2.5–12.5 eV) and high-energy (50–75 eV) parts of the electron spectrum. These differences were attributed to different weightings of isomeric atoms on or near the surface of the collector and deeper within the collector material.

Still more recent results of Nève de Mévergnies (203) have been obtained with ^{235m}U collection and decay within the same vacuum system. There seems to be a correlation between the decay rate and the free-electron density. When metals of group Ib, such as Cu, Ag, and Au, are used as hosts, the experimental values of the decay constant λ are consistent with a proportionality to the 1/12 power of the free-electron density, as would be expected from a screened-potential model. The latest data are shown in Figure 4. A similar dependence on atomic concentration can be seen for elements of Group VIII (bivalent Ni and Pt and trivalent Co and Ir) and of Group IVb (Ti and Hf). For metals whose valence is closer to that of uranium the dependence on atomic concentration is weaker.

Measurements with such low energy electrons are extremely difficult, but the size of the effects found, and—if the transition energy is between about 50 and 100 eV—the simplicity of the conversion process, make this case potentially a very fruitful one.

3.11 OTHER CASES

²³⁹Pu, ²³³U.—Novakov & Hollander (204) initiated a series of measurements of the effects of strong electric fields on the shapes, positions, and relative intensities of internal conversion and photoelectric conversion lines. Since this work has already been reviewed (21), we comment only briefly on the chemical effects involved. In the presence of a macroscopic field of the order of 10⁷V/cm the *L*₃ internal conversion line of the 57.2-keV transition of ²³⁹Pu, following decay

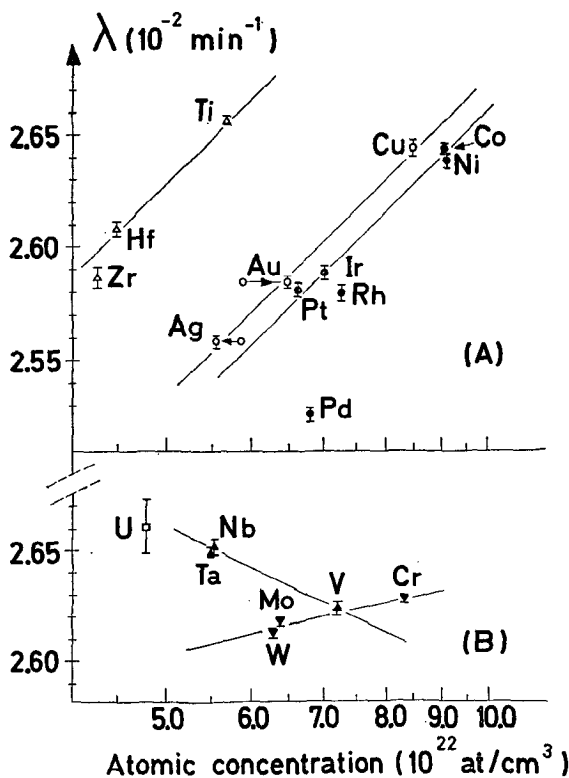


FIGURE 4. Results of Nève de Mévergnies (203) for the decay constant of ^{235m}U implanted in various transition metals, vs atomic concentration of the host. Part (A) includes the low-valence hosts, and part (B) those hosts with valence 5 or 6. For Ag and Au the data points without error bars are plotted at the nominal atomic concentrations, while those with error bars are plotted at an equivalent concentration deduced from free-electron densities as derived from Hall-effect measurements.

of ^{239}Np , was found to be shifted by about 100 keV, while the L_2 line was unshifted; the shifts were observed with chloride and oxide sources, but not with sources in the hydroxide form (205). Further studies with the outer-shell conversion lines of the ^{239}Pu 7.85-keV line were also reported (206–207). Changes in the relative intensity of the N_1 line, relative to N_2 and N_3 , between oxide and hydroxide sources, were observed (207). The work on line shifts and shapes was continued with photoelectron spectroscopy (206, 208).

^{134}Cs .—Studies of the internal conversion spectrum of the 11.23-keV transition, with sources of ^{134m}Cs (3 hr), have been undertaken by Martin & Schulé (209). The transition is magnetic dipole, with a very small $E2$ admixture. Spec-

trometer resolutions of about 0.1% were used. Sources in the chemical forms CsI, CsBr, and Cs₂SO₄ were studied. Differences in the relative amounts of discrete energy loss were found. No evidence for *P*-shell conversion was found with any of the sources.

⁶⁴Cu.—Kemeny (210) has reported studies of half-life changes of this nucleus, between sources in the metallic form and sources in sulphate and ammonium sulphate solutions. ⁶⁴Cu has a half-life of 12.8 hr, and decays by negatron emission (40%), positron emission (19%), and electron capture (41%). All decays are allowed (211). A NaI spectrometer observed the annihilation quanta and gamma-rays. The results reported were:

$$\begin{aligned}\lambda(\text{CuSO}_4 \text{ soln.}) - \lambda(\text{Cu}) &= (1.70 \pm 0.64)10^{-2}\lambda(\text{Cu}) \\ \lambda[\text{Cu}(\text{NH}_3)_4\text{SO}_4 \text{ soln.}] - \lambda(\text{Cu}) &= - (0.87 \pm 0.30)10^{-2}\lambda(\text{Cu})\end{aligned}$$

The magnitude of the effects is somewhat surprising.⁴

¹³¹I.—Comparisons of the decay of ¹³¹I in the chemical form NaI, between sources in solution and the solid salt, were carried out by Bergamini et al (212). Effects of a few percent were reported. Similar investigations were performed by Kemeny (213), who found a fractional rate difference of $4.3 \pm 2.1\%$. In both cases the half-life was apparently longer for the source in solution. The situation has now been studied in detail by Zoller et al (214). The half-life of ¹³¹I is 8.0 days. In 1.5% of decays (215) the 12-day daughter activity ^{131m}Xe is formed. With a thin-window counter, sensitive to the radiations of ^{131m}Xe, the apparent ¹³¹I half-life was about 2% longer than when an absorber was present. Sources in a variety of physical and chemical forms were studied. When the contribution of ^{131m}Xe was accounted for, no differences in half-life greater than 0.3% were observed. It was concluded by Zoller et al that the previous results (212, 213) do not establish the presence of chemical effects on the half-life of ¹³¹I. See also (274).

4. MACROSCOPIC WAYS OF CHANGING THE RATES OF ELECTRON CAPTURE AND INTERNAL CONVERSION

4.1 CHEMICAL STATE

If atoms entered purely ionic bonds, with valence electrons completely transferred from one partner to another, the changes in electron density near the nucleus important for the rates of capture and conversion would be relatively large and easily estimated. That the situation is considerably more complicated than this was recognized already in the initial suggestion of the ⁷Be experiment (6). Even if in Be metal the valence electrons are in *p* as well as *s* bands, the difference in electron density at the nucleus in going to double-ionized Be should

⁴ A careful comparison of the half-life of ⁶⁴Cu, between the chemical forms copper and copper oxide, has recently been made by Johnson & Harbottle (211a), with the result $\Delta\lambda/\lambda = (0 \pm 3)10^{-4}$. See also (274).

be of the order of one percent. Yet the half-life difference found between Be metal and BeF_2 was only 0.08%.

That the near-nuclear valence electron density decreases when a metal atom forms an ionic bond is shown directly by the ^{119}Sn experiment (Sec. 3.6); that the SnO_2 $5s$ conversion was only 30% less than that for Sn metal exemplifies the kind of renormalization of the formal valence state which must be taken into account. The apparent absence of Cs $6s$ conversion in Cs halides and sulphate (Sec. 2.11) may indicate that the effects are simpler in simpler atoms.

In addition to effects directly related to bond ionicity, or electronegativity of bonding partners, one must expect effects of bond length, as first discussed by Slater (17), in connection with the result that the 2.2-keV transition in ^{99}Tc decays faster in KTcO_4 than in Tc metal. The significance of bond lengths for the extensive ^7Be results has been discussed by Johlige et al (113).

There are many low-energy isomeric transitions whose rates are not dominated by s -state conversion. Low-energy $E2$ and $E3$ transitions, for example, convert almost entirely in p -states. $M2$ and $M3$ transitions often have comparable amounts of conversion in s - and p -states. With higher multipole order, d -state conversion can become an appreciable part of the total. One has the opportunity, then, of studying transitions for which the electrons taking part in the chemical bonding are not important for the conversion, as well as cases where the bonding electrons are important for the conversion. While the bonding electrons will respond directly to the chemical perturbation (near-nucleus densities decreasing with ionic bond charge transfer away from the atom, or with increasing ionic radius), outer-shell electrons not participating in the bonding may often react the other way, due to changes in their screening from the nucleus by the bonding electrons. This sort of effect (24) provides an alternative explanation for the ^{99}Tc results (Sec. 3.5), since the Tc valence electrons are s and d , while the $E3$ transition converts mostly in p -states.

Chemical effects on the total electron density at the nucleus have been studied in detail by use of the isomeric chemical shift in the Mössbauer effect (20). The magnitude of this shift—isomer shift for short—is proportional to both the change in electron density at the nucleus between source and absorber, and to the change in mean-square radius of the nucleus between the ground and isomeric state. For chemical effects on conversion and capture rates there is no complicating radius-change factor. For those decay modes whose rates are directly proportional to electron density at the nucleus (most electron captures and $M1$ internal conversion, for example) there should be a direct correlation with the isomer shift. Results of the two kinds of experiment may be combined to give the nuclear radius-change parameter (19, 123, 126, 167, 216), the more difficult rate-change experiments thus serving as a calibration for the often extensive isomer shift data.

So far, however, no successful experiment has been completed⁵ which gives directly a total capture or conversion rate change which can be used to calibrate a set of measured isomer shifts. The method of chemical perturbation of valence-

⁵ The new work mentioned in footnote 3 is the first such case.

shell conversion probably will give results which are accurate enough for most purposes. Its application to isomer-shift calibration, however, requires an assumption about the response of the inner shells to a chemically-induced change in valence-electron near-nuclear density. If $\Delta\rho(0)$ and $\Delta\rho_v(0)$ are the changes in total and valence density at the nucleus, they may be related thus:

$$\Delta\rho(0) = \Delta\rho_v(0)(1 + M) \quad 21.$$

$$M = \sum_{i < v} \frac{d\rho_i(0)}{d\rho_v(0)} \quad 22.$$

We may call M the monopole shielding factor. Estimates of M by the Crawford-Schawlow method (217) and by inspection of nonrelativistic Hartree-Fock results lead to values such as $M = -0.15$ (19). Inspection of relativistic Hartree-Fock results, however, leads in some cases to much smaller corrections (167, 218, 219). It would seem interesting to explore, both theoretically and experimentally, how important monopole shielding is. The concept of monopole shielding, defined here for s -electrons, is easily extended to other orbital quantum numbers and to combinations, and is analogous to the magnetic dipole shielding of Lamb (220) and the quadrupole shielding of Sternheimer (221-223).

The possibility of studying total radioactive rate changes for a variety of internal conversion and electron capture transitions, changes in internal conversion spectra, and Mössbauer-effect isomer shifts, all for the same element in different chemical forms, and correlating the results with inner-shell binding-energy changes (21, 115), may lead to a major increase in fundamental understanding of real chemical bonds. The results so far, at least concerning the prediction and explanation of decay rate perturbations, have been at best semi-quantitative.

4.2 PRESSURE

With increasing pressure, valence-electron densities in the region of the nucleus generally increase, thus increasing most capture and conversion decay rates. Experiments of this type have been done with ^{99}Tc (150, 151) and ^{90}Nb (146), and estimates of the expected size of the effect have been made by Porter & McMillan (152). In addition to the direct squeezing of the wavefunctions, a pressure increase can result in transfer of electrons from one band to another (for example, from an s band to a d band); such effects are important in the analysis of pressure-induced isomer shifts (224-226).

4.3 SUPERCONDUCTIVITY

Gentle as the superconducting transition is, its effects on total internal conversion rates have apparently been observed in the cases of ^{99}Tc (149) and ^{90}Nb (145). In both cases the samples were held at 4.2°K, and comparisons were made with and without an applied magnetic field large enough to destroy superconductivity. The effects were relatively large, 0.5×10^{-3} and 2.0×10^{-3} , respectively, and of opposite sign. The application of the magnetic field decreased the rate in Tc and increased it in Nb. In both cases s and d valence electrons are available

for conversion. The difference in sign of the effect is probably related to the dominance of p -electron conversion in the $E3$ Tc transition, in contrast to the more or less equal contribution of $s_{1/2}$ and $p_{3/2}$ bound states in the $M2$ Nb transition. It is possible, but less likely, that the change in occupancy of the $4d$ orbital, from less than half-filled in Nb metal to more than half-filled in Tc metal, is relevant. No convincing explanation of the magnitudes of the effects has been presented. An experiment by Snyder (227) on the temperature dependence of the ^{119}Sn Mössbauer-effect isomer shift did not show a discontinuity across the superconducting phase transition, but the upper limit is not inconsistent with the rate-change effects (24).

4.4 INTERNAL ELECTRIC AND MAGNETIC FIELDS

An influence of the ferroelectric phase transition of barium titanate on the decay rate by electron capture and internal conversion of active atoms substituted in the crystal, has been observed for ^{85}Sr (135), ^{89}Zr (134), and $^{99\text{m}}\text{Tc}$ (154). In all three cases the decay was slower in the ferroelectric phase. The effect was very small for ^{85}Sr , about 0.8×10^{-3} for ^{89}Zr , and about 2.6×10^{-3} for ^{99}Tc , where only outer electrons contribute to the decay. In all cases it was thought that the active atoms occupied titanium sites.

In passing from the cubic paraelectric phase to the tetragonal ferroelectric phase the lattice constants of BaTiO_3 change (228), and the heavy ions undergo additional shifts, of the order of 0.1 Å, relative to the oxygen ions (229). These changes in bond lengths are probably sufficient to account for the observed rate changes. The influence of the internal electric fields is more difficult to estimate. Estimates of the strength of these fields run up to a few times 10^9 V/cm in the spaces between the atoms (230). Electrons are very efficient at screening electric fields from the inner atom region (231), so the effect will be mostly on the valence electrons. Stark-effect mixing of the bound levels results, in first order, only in a redistribution of the capture or conversion, leaving the total rate unchanged. A possible effect of continuum-state mixing on the conversion rate does not seem to have been considered yet.

An experiment on the effect of the dielectric field in a condenser on the decay rate of $^{99\text{m}}\text{Tc}$ has also been performed (153). With macroscopic fields of the order of 2×10^4 V/cm, the effects were of the order of 10^{-4} .

Internal conversion spectra of sources in strong macroscopic electric fields show line shifts, and line-shape changes (204–207), and sometimes apparent redistributions of intensity within multiplets (207); the effects are dependent on the chemical form of the source. The line-shift results, together with similar results from photoelectron spectroscopy (208), are at least partly understood (21).

Strong magnetic fields should induce splittings of internal conversion lines. Such splittings are seen in photoelectron spectroscopy (129). Since magnetic field effects are mostly diagonal, it is unlikely that observable changes in total capture or conversion rates can be produced by available magnetic fields. Core polarization effects in iron have been studied by Song et al (130), who used resonance excitation with polarized gamma-rays.

4.5 TEMPERATURE

Except in the vicinity of phase transitions, such as have just been discussed, the effects of temperature changes on capture and conversion rates should be of modest size, and may be characterized in much the same way as temperature-dependent Mössbauer isomer shifts (168, 227). The volume effect, due to thermal expansion, will be similar to that found in pressure studies. There may be specific effects of changing rms vibrational amplitude, from squeezing of wavefunctions and, in polar environments, from high-frequency electric fields. The purely kinematic effect of second-order Doppler shift (232, 233) will play a much smaller role here than for the isomer shift.

Byers & Stump (149) have compared the ^{99m}Tc decay rate at room temperature with that for "normal" Tc metal at 4.2°K, and found an effect of about one part in 10^4 , with the decay faster at the low temperature.

4.6 PLASMAS

Ionization of the atom would be a direct way of altering the rates of electron capture and internal conversion decays. Matter in stellar interiors is ionized, in general, with charge compensation by an electron gas. As noted in Sec. 2.1, the effects of the ionization and of the capture of free electrons (53, 54) have been considered. Alterations of the decay rate of ^7Be and the resulting changes in the expected solar neutrino flux have been studied by Bahcall (234) and by Iben et al (235). The rate of ^3He electron capture, under stellar conditions, has been discussed by Schatzman (236). Internal conversion plays a much smaller role in stellar development.

Internal conversion in ionized atomic systems can be important in certain realizable laboratory conditions, however. Valadres, Walen & Briancon (237) reported differences in conversion line shapes between lines due to the 29.9- and 31.6-keV transitions in ^{223}Ra following alpha decay of ^{227}Th . Detailed studies of the differences have been made by Gelletly, Geiger & Merritt (238). Most of the feeding of the 61.5-keV level, from which the 31.6-keV transition proceeds, is by direct alpha decay. Even those Ra atoms which recoil out of the source into vacuum have a mean charge state of only +1. About two-thirds of the 29.9-keV transitions, on the other hand, are preceded by an internally converted transition, which leads to a mean charge state of about +12 for those which have recoiled into vacuum. The resulting binding-energy shift for the *L* and *M* shells was found (238) to be about 200 eV, with a rather broad distribution showing the contribution of several charge states. One would expect a corresponding decrease in outer-shell conversion and a small (of the order of a part per thousand) increase in the transition half-life.⁶ Such effects may possibly play

⁶ Walen, Valadres & Briancon (238a) have recently reported a measurement of the change in half-life of the 59.5 keV state of ^{237}Np between highly-charged (average of ~ 14 units) and weakly-charged (< 5 units) recoil ions from ^{241}Am alpha decay; the result was $\Delta\lambda/\lambda = (3 \pm 2) 10^{-3}$.

some role in work on internal conversion from heavy ions recoiling from nuclear reactions.

That atomic systems, even in a solid environment, do not always recover from preceding transitions in time to present normal surroundings for a subsequent decay, is shown by the existence of monoenergetic positron emission. This effect, predicted by Sliv (239), and for which further calculations have been made (240), has been observed in a few cases (241, 242). Incomplete recovery from preceding transitions also has effects on angular correlations (243).

5. SPECULATIONS AND POSSIBILITIES

5.1 ALPHA DECAY, BETA DECAY, AND FISSION

Alpha decay and fission.—Alpha-decay rates are greatly sensitive to the difficulties of penetration through the Coulomb barrier surrounding the nucleus. This barrier is slightly different for nuclei surrounded by their electron cloud than it would be for bare nuclei. Chemical or other environmental effects on the electron cloud can slightly perturb the barrier and thus affect the decay rate. The problem was formulated by Alder, Baur & Raff (244) in terms of changes in the electron screening potential, ΔV^S . In the approximation of a constant ΔV^S through the barrier they derived the relation

$$\Delta\lambda/\lambda = 3.97 \times 10^{-6} (1 - 4/A)^2 (Z - 2) [E(\text{MeV})]^{-8/2} [V^S(\text{eV})] \quad 23.$$

which involves the further approximation, shown by them to be good, that only the leading, or Gamow, term is kept in the penetration-factor exponent.

In estimating practicable values of ΔV^S it must be kept in mind that it is not changes in the constant potential in the barrier region, due to the electrons outside, which affects the penetration, but changes in that part of the potential due to electron charge density inside the nucleus and within the barrier region. An upper limit for the effect can thus be obtained by using for ΔV^S that difference in potential due to electrons between the inner and outer classical turning points which can be changed in a chemical reaction. For illustrative purposes we consider the alpha decay of ^{226}Ra . The difference between the classical turning points of the total potential due to electrons can be taken from the relativistic Hartree-Fock-Slater tabulation of Carlson et al (245), and is 124 eV. The fraction of this potential difference due to valence ($7s$) electrons may be derived from the tables of Herman & Skillman (111), supplemented for the inner shells by Behrens & Jänecke (31), and is 3.9×10^{-5} . The expected upper limit on the chemical shift in effective screening potential is then only 4.8×10^{-3} eV, leading, for this case, to an expected fractional rate change of $\Delta\lambda/\lambda = 1.5 \times 10^{-7}$.⁷

Similar estimates can be made for spontaneous fission, and also lead to estimated perturbations which are very small.

⁷ A more precise evaluation of the effect has now been reported by Rubinson & Perlman (245a); for the case of ^{147}Sm their estimate of the order of magnitude of chemical effects is $\Delta\lambda/\lambda \approx 7 \times 10^{-8}$.

Beta decay.—Screening also affects the rate of beta decay, whether electron or positron decays are considered. Small corrections for screening are important in the evaluation, from intra-multiplet decays in light nuclei, of the Fermi coupling constant (246, 247). Predictions of the total screening effect, due to all the atomic electrons, are given in graphical form by Behrens & Jänecke (31); this total effect rises to the order of 4% for electron emission from heavy nuclei, and is even higher for positron emission at high Z when the maximum kinetic energy is low. The fraction of this screening effect that can be changed in a chemical reaction has been estimated by Alder, Baur & Raff (248), who conclude that in typical cases the effects might be a few parts in 10^4 , with slightly larger effects possible for low-energy negatron decays at low Z and low-energy positron decays at high Z . The expected effects are then considerably smaller than those reported for ^{64}Cu and ^{131}I (Sec. 3.11).

Atomic and chemical effects on the tritium beta spectrum have been discussed by Bergkvist (249). Among the most interesting points are a smearing out of the end-point energy, due to the variety of atomic final states, and a re-evaluation of the screening potential, involving an increase of about 50%. The exclusion-principle inhibition of beta decay in stellar interiors, due to the number of continuum electron states already occupied, was discussed by Bahcall (54).

The beta decay of ^{187}Re is an especially interesting candidate for study because of its low end-point energy. The most recent values are 2.62 ± 0.09 keV (250) and 2.65 ± 0.04 keV (251). That this decay occurs at all is an example of the effects of the atomic environment on nuclear decay: the bare nucleus ^{187}Re is stable against beta decay and it is the difference of 15 keV in the total electronic binding energy of osmium and rhenium (245) which makes the decay possible. Direct half-life change experiments would be, of course, very difficult since the half-life is so long—of the order of 5×10^{10} years (252)—and the specific activity therefore so small.

5.2 GAMMA-RAY EMISSION AND HIGHER-ORDER PROCESSES

Gamma-ray emission rates must, in principle, be affected by the presence of the atomic electron cloud. Changes in the electron cloud can then affect the decay rates. The total effect of the atomic electrons on gamma-emission rates has been considered by Krutov & Fomenko (253, 254). Typical results for the 44-keV $E2$ ^{238}Pu and 18.5-keV $E3$ ^{124}Sb transition were 0.040% and 0.017%, respectively. For the low-energy $E3$ transition in ^{235}U , (Sec. 3.10), however the photon-decay rate was increased by a factor of more than two (for an assumed transition energy of 75 eV—the effect is even larger if the energy is lower).

The contribution of higher-order terms to internal conversion rates was studied by Hager & Seltzer (79) for L_1 conversion of $E2$ transitions. Krutov & Knyazkov (255) have presented estimates of higher-order effects for a number of cases. Effects of interaction with the electron cloud on the analysis of experiments on the relative phase of multipole components in a mixed transition have been considered by Hannon & Trammell (256) [see also the review of Henley (257)].

Penetration effects in conversion (56, 58, 258–260) enter as amplitudes which are directly proportional to the bound-state radial amplitudes in the nucleus. They are appreciable only for retarded transitions where second-order effects may be especially important.

All these effects are small enough that measurable external perturbation will require reasonably exotic circumstances.

5.3 OTHER POSSIBILITIES

Coupling-constant changes.—Changing the coupling constant responsible for a decay process is a direct way of changing the decay rate. If the weak-interaction coupling constant g of Equation 1 changed, for example, the M^2 factor (Equation 20) would change, perturbing all beta-decay and electron-capture rates. Similarly, changes in e , the electromagnetic coupling constant, would change gamma-ray and internal conversion rates. Even more dramatic effects could come from the kinematic effects of changes in e . Changes in time of fundamental constants, such as e and g , have been discussed from time to time, for example, by Dirac (261, 262), and by Gamow (263). Among the best evidence that such changes have been very small is that coming from the discussion of kinematic shifts in alpha decay rates by Wilkinson (264), and from Dyson's discussion (265) of the effect of such a change in e on the Q -value of ^{187}Re beta decay (see above). On the other hand, a recent re-examination by Spector (266) of data on pleochroic halos led to the conclusion that those data do not provide convincing proof that the laws of radioactive decay are constant in time.

Other reported effects.—Speculations on whether nuclear processes can be stimulated by the electronic structure of macromolecules have been presented by Konarski, Wszolek & Kukiel (267), in connection with their reported observation of the emission of electrons, protons, and deuterons by biological materials (268–270). Alterations of the radioactive decay process by chemical and electrostatic means, as shown by apparent deviations from Poisson statistics, have been reported by Anderson & Spangler (271).

ACKNOWLEDGMENT

I wish to thank a large number of colleagues, at Brookhaven, Indiana, and elsewhere, and especially E. L. Church and M. L. Perlman, for discussions, enlightenments, and access to new data.

LITERATURE CITED

1. Meyer, S., Schweidler, E. 1927. *Radioaktivität*. Leipzig: B. G. Teubner. 2nd ed.
2. Kohlrausch, K. W. F. 1928. *Radioaktivität, Handbuch der Experimentalphysik*, Vol. 15. Leipzig: Akademische Verlagsgesellschaft mbH
3. Bothe, W. 1933. *Handbuch der Physik* ed. H. Geiger, K. Scheel, Vol. 22-1, 201-244. Berlin: Springer. 2nd ed.
4. Curie, M., Kamerlingh Onnes, M. 1913. *Le Radium* 10:181
5. Rutherford, E., Petavel, J. E. 1907. *Brit. Assoc. Advan. Sci., Rep. A* p. 456; Rutherford, E. 1963. *Collected Papers*, Vol. 2, p. 36. New York: Interscience
6. Segrè, E. 1947. *Phys. Rev.* 71:274
7. Daudel, R. 1947. *Rev. Sci.* 85:162
8. Bouchez, R., Daudel, R., Daudel, P., Muxart, R. 1947. *J. Phys. Radium* 8:336
9. Bouchez, R., Daudel, P., Daudel, R., Muxart, R. 1948. *C. R. Acad. Sci.* 227:525
10. Bouchez, R., Daudel, P., Daudel, R., Muxart, R., Rogozinski, A. 1949. *J. Phys. Radium* 10:201
11. Segrè, E., Wiegand, C. E. 1949. *Phys. Rev.* 75:39, 81:284
12. Leininger, R. F., Segrè, E., Wiegand, C. E. 1949. *Phys. Rev.* 76:897, 81:280
13. Kraushaar, J. J., Wilson, E. D., Bainbridge, K. T. 1953. *Phys. Rev.* 90:610
14. Bouchez, R. et al 1956. *J. Phys. Radium* 17:363
15. Bainbridge, K. T., Goldhaber, M., Wilson, E. 1951. *Phys. Rev.* 84:1260
16. Ibid 1953. 90:430
17. Slater, J. C. 1951. *Phys. Rev.* 84:1261
18. Cooper, J. A., Hollander, J. M., Rasmussen, J. O. 1965. *Phys. Rev. Lett.* 15:680
19. Bocquet, J.-P., Chu, Y. Y., Kistner, O. C., Perlman, M. L., Emery, G. T. 1966. *Phys. Rev. Lett.* 17:809
20. DeBenedetti, S., Barros, F. DeS., Hoy, G. R. 1966. *Ann. Rev. Nucl. Sci.* 16:31
21. Hollander, J. M., Shirley, D. A. 1970. *Ann. Rev. Nucl. Sci.* 20:435
22. Daudel, R. 1952. *J. Phys. Radium* 13:557
23. Perlman, M. L. 1969. *Vistas in Research*, Vol. 4, p. 171. New York: Gordon and Breach
24. Perlman, M. L., Emery, G. T. 1969. *Proc. Int. Conf. on Radioactiv. in Nucl. Spectrosc.*, ed. J. H. Hamilton, J. C. Manthuruthil. New York: Gordon and Breach
25. Konopinski, E. J. 1966. *The Theory of Beta Radioactivity*. London: Oxford Univ. Press
26. Schopper, H. F. 1966. *Weak Interactions and Nuclear Beta Decay*. Amsterdam: North-Holland
27. Wu, C. S., Moszkowski, S. A. 1966. *Beta Decay*. New York: Interscience-Wiley
28. Bouchez, R., Depommier, P. 1960. *Rep. Prog. Phys.* 23:395
29. Berenyi, D., Ed. 1968. *Proc. Conf. Electron Capture and Higher Order Processes in Nucl. Decays, Debrecen, Hungary, July 15-18, 1968*. Budapest: Eötvös Lorand Phys. Soc.
30. Berenyi, D. 1968. *Rev. Mod. Phys.* 40:390
31. Behrens, H., Jänecke, J. 1969. *Landolt-Börnstein Numerical Tables for Beta-Decay and Electron Capture*, ed. K.-H. Hellwege, H. Schopper, Vol. 4., Group 1. Berlin: Springer-Verlag
32. Bühring, W. 1963. *Nucl. Phys.* 40:472
33. Ibid 49:190
34. Stech, B., Schülke, L. 1964. *Z. Phys.* 179:314
35. Bühring, W., Schülke, L. 1965. *Nucl. Phys.* 65:369
36. Behrens, H., Bühring, W. 1971. *Nucl. Phys. A* 162:111
37. Bahcall, J. N. 1962. *Phys. Rev. Lett.* 9:500
38. Bahcall, J. N. 1963. *Phys. Rev.* 129:2683
39. Ibid 131:1756
40. Ibid 132:362
41. Bahcall, J. N. 1965. *Nucl. Phys.* 71:267
42. Benoist-Gueutal, P. 1963. *Ann. Phys. Paris* 8:593
43. Odier, S., Daudel, R. 1956. *J. Phys. Radium* 17:60
44. Moler, R. B., Fink, R. W. 1963. *Phys. Rev.* 131:821
45. Genz, H. 1972. *Proc. Int. Conf. on Inner-Shell Ionization Phenomena*. Amsterdam: North-Holland

46. Lark, N. L., Perlman, M. L. 1960. *Phys. Rev.* 120:536
47. Carlson, T. A., Nestor, C. W., Jr., Tucker, T. C., Malik, F. B. 1968. *Phys. Rev.* 169:27
48. Serber, R., Snyder, H. S. 1952. *Phys. Rev.* 87:152
49. Erman, P., Sigfridsson, B., Carlson, T. A., Fransson, K. 1968. *Nucl. Phys. A* 112:117
50. der Mateosian, E. 1971. *Phys. Rev. A* 3:573
51. Stephas, P., Crasemann, B. 1967. *Phys. Rev.* 164:1509
52. Crasemann, B., Stephas, P. 1969. *Nucl. Phys. A* 134:641
53. Bethe, H., Bacher, R. F. 1936. *Rev. Mod. Phys.* 8:82
54. Bahcall, J. N. 1962. *Phys. Rev.* 126:1143
55. Bohr, A., Weisskopf, V. F. 1950. *Phys. Rev.* 77:94
56. Church, E. L., Weneser, J. 1960. *Ann. Rev. Nucl. Sci.* 10:193
57. Rose, M. E. 1958. *Internal Conversion Coefficients*. Amsterdam: North-Holland
58. Church, E. L. 1966. *Brookhaven Nat. Lab. Rep. BNL 50002 (T-428)*
59. Rose, M. E. 1965. *Alpha-, Beta-, and Gamma-Ray Spectroscopy*, ed. K. Siegbahn, p. 887. Amsterdam: North-Holland
60. Listengarten, M. A. 1961. *Gamma-Luchi*, ed. L. A. Sliv, p. 271. Moscow: Akademii Nauk SSSR
61. Hamilton, J. H., Ed. 1966. *Internal Conversion Processes*. New York: Academic
62. Sliv, L. A., Band, I. M. 1965. *Alpha-, Beta-, and Gamma-Ray Spectroscopy*, ed. K. Siegbahn, p. 1939. Amsterdam: North-Holland
63. Hager, R. S., Seltzer, E. C. 1968. *Nucl. Data A* 4:1
64. Pauli, H. C. 1967. *Purdue Univ. Rep. COO-1420-137*
65. Dragoun, O., Pauli, H. C., Schmutzler, F. 1969. *Nucl. Data A* 6:235
66. Bhalla, C. P. 1966. *Nucl. Phys.* 82:433
67. Bhalla, C. P. 1966. *Bases for Nuclear Spin-Parity Assignments*, ed. N. B. Gove, R. L. Robinson, p. 104. New York: Academic
68. Bhalla, C. P. 1966. *Z. Phys.* 196:26
69. Bhalla, C. P., Freedman, M. S., Porter, F. T., Wagner, F. 1966. *Phys. Lett.* 23:116
70. Bhalla, C. P. 1967. *Phys. Rev.* 157:1136
71. Pauli, H. C. 1968. *Niels Bohr Inst. Rep.*
72. Sliv, L. A. 1951. *Zh. Eksp. Teor. Fiz.* 21:770
73. Sliv, L. A., Listengarten, M. A. 1952. *Zh. Eksp. Teor. Fiz.* 22:29
74. Hager, R. S., Seltzer, E. C. 1967. *Calif. Inst. Tech. Rep. CALT-63-60*
75. Erman, P., Emery, G. T., Perlman, M. L. 1966. *Phys. Rev.* 147:858
76. Karlsson, S. E. et al 1966. *Nucl. Phys.* 89:513
77. Gelletly, W., Geiger, J. S., Graham, R. L. 1967. *Phys. Rev.* 157:1043
78. Dingus, R. S., Rud, N. 1968. *Nucl. Phys. A* 117:73
79. Hager, R., Seltzer, E. 1970. *Phys. Rev. C* 2:902
80. Goldhaber, M., Sunyar, A. W. 1951. *Phys. Rev.* 83:906
81. Mihelich, J. W. 1952. *Phys. Rev.* 87:646
82. Swan, J. B., Hill, R. D. 1953. *Aust. J. Phys.* 6:371
83. Graham, R. L. 1966. *Bases for Nuclear Spin-Parity Assignments*, ed. N. B. Gove, R. L. Robinson, p. 53. New York: Academic
84. Church, E. L., Schwarzschild, A., Weneser, J. 1964. *Phys. Rev. B* 133:35
85. Carroll, C. O., O'Connell, R. F. 1966. *Nucl. Phys.* 80:500
86. Moragues, J. A., Gelletly, W., Mariscotti, M. A. J. 1968. *Phys. Lett. B* 27:441
87. Church, E. L. 1968. *Phys. Lett. B* 28:168
88. Church, E. L. 1965. Private communication
89. Band, I. M., Sliv, L. A., Trzhaskovskaya, M. B. 1970. *Nucl. Phys. A* 156:170; *Zh. Eksp. Teor. Fiz. Pizma Red.* 11:306 (*JETP Lett.* 11:201)
90. Berestetski, V. B. 1948. *Zh. Eksp. Teor. Fiz.* 18:1070
91. Drell, S. D. 1949. *Phys. Rev.* 75:132
92. Church, E. L., Monahan, J. E. 1955. *Phys. Rev.* 98:718
93. Slichter, C. P. 1963. *Principles of Magnetic Resonance*, 86-89. New York: Harper & Row
94. Fermi, E. 1930. *Mem. Reale Accad. Ital. Cl. Sci. Fis. Mat. Natur. Fis.* 1.139; 1930. *Z. Phys.* 60:320; 1962. *Collected Papers*, Vol. I, p. 336. Chicago: Univ. Chicago Press
95. Fermi, E., Segrè, E. 1933. *Z. Phys.* 82:11,729; 1933. *Mem. Reale Accad. Ital. Cl. Sci. Fis. Mat. Natur. Fis.* 4:131; 1962. Fermi, E.

- Collected Papers*, Vol. I, p. 514. Chicago: Univ. Chicago Press
96. Olsson, O. M., Hultberg, S. 1959. *Ark. Fys.* 15:361
 97. Daniel, H. 1969. *Z. Phys.* 223:150
 98. Pratt, R. H., Tseng, H. K. 1972. *Phys. Rev. A* 5:1063
 99. Bocquet, J.-P., Chu, Y. Y., Emery, G. T., Perlman, M. L. 1968. *Phys. Rev.* 167:1117
 100. Dragoun, O., Jahn, P., Allers, H., Vobecky, M., Daniel, H. 1968. *Phys. Lett. B* 28:251; MPIH-1968. No. V11. Heidelberg: Max-Planck-Institute für Kernphysik
 101. Pleiter, F. 1971. *Nucl. Phys. A* 163:425
 102. Fujioka, M. et al 1971. Private communication
 103. Church, E. L. 1967. *Bull. Am. Phys. Soc.* 12:904
 104. Pauli, H. C. 1968. *Nucl. Phys. A* 109:94
 105. Dragoun, O., Plajner, Z., Schmutzler, F. 1969. Rep. MPIH-1969 No. V5. Heidelberg: Max-Planck-Institut für Kernphysik
 106. Anderson, E. M., Listengarten, M. A., Khanokind, M. A. 1970. *Izv. Akad. Nauk SSSR Ser. Fiz.* 34:850 (*Bull. Acad. Sci. USSR Phys. Ser.* 34:757)
 107. Porter, F. T., Freedman, M. S., Wagner, F., Jr. 1971. *Phys. Rev. C* 3:2246
 108. Porter, F. T., Freedman, M. S. 1971. *Phys. Rev. C* 3:2285
 109. Moore, C. E. 1949. *Atomic Energy Levels, Vols. I-III. Nat. Bur. of Stand. Circ.* 467
 110. Lauritsen, T., Ajzenberg-Selove, F. 1966. *Nucl. Phys.* 78:1, especially p. 45-47
 111. Herman, F., Skillman, S. 1963. *Atomic Structure Calculations*. Englewood Cliffs: Prentice-Hall
 112. Bainbridge, K. T., Baker, E. 1959. *Bull. Am. Phys. Soc.* 4:278
 113. Johlige, H. W., Aumann, D. C., Born, H.-J. 1970. *Phys. Rev. C* 2:1616
 114. Hamrin, K., Johansson, G., Fahlman, A., Nordling, C., Siegbahn, K. 1967. *Univ. Uppsala Inst. Phys. Rep. UUIP-548*
 115. Siegbahn, K. et al 1967. *ESCA: Atomic, Molecular and Solid State Structure Studied by Means of Electron Spectroscopy*, 76-77. Stockholm: Almqvist & Wiksells
 116. Jacques, R. 1956. *Cahiers de physique Nos. 70:1 71-72:23 75-76:18*
 117. Mössbauer, R. L. 1962. *Ann. Rev. Nucl. Sci.* 12:123
 118. Rapaport, J. 1970. *Nucl. Data B* 3(3,4):103
 119. Kistner, O. C., Šunyar, A. W. 1960. *Phys. Rev. Lett.* 4:412
 120. Walker, L. R., Wertheim, G. K., Jaccarino, V. 1961. *Phys. Rev. Lett.* 6:98
 121. Šimánek, E., Šroubek, Z. 1967. *Phys. Rev.* 163:275
 122. Šimánek, E., Wong, A. Y. C. 1968. *Phys. Rev.* 166:348
 123. Pleiter, F., Kolk, B. 1971. *Phys. Lett. B* 34:296
 124. Fujioka, M., Hisatake, K. 1972. *Phys. Lett. B* 40:99
 125. Verma, R. N., Emery, G. T. 1972. *Bull. Am. Phys. Soc.* 17:545
 126. Raff, U., Alder, K., Baur, G. 1972. *Helv. Phys. Acta*, Vol. 45
 - 126a. Ruesegger, R., Kündig, W. 1972. *Phys. Lett. B* 39:620
 127. Hanna, S. S., Heberle, J., Perlow, G. J., Preston, R. S., Vincent, D. H. 1960. *Phys. Rev. Lett.* 4:513
 128. Watson, R. E., Freeman, A. J. 1961. *Phys. Rev.* 123:2027
 129. Fadley, C. S., Shirley, D. A., Freeman, A. J., Bagus, P. S., Mallow, J. V. 1969. *Phys. Rev. Lett.* 23:1397
 130. Song, C. J., Trooster, J. M., Benczer-Koller, N., Rothberg, G. M. 1972. *Bull. Am. Phys. Soc.* 17:87
 131. Morita, M., Sugimoto, K., Yamada, M., Yokoo, Y. 1969. *Progr. Theor. Phys.* 41:996
 132. Yokoo, Y., Kodama, T., Morita, M. 1970. *Progr. Theor. Phys.* 44:294
 133. Johns, M. W., Park, J. Y., Shafroth, S. M., Van Patter, D. M., Way, K. 1970. *Nucl. Data A* 8:373
 134. Gagneux, S., Huber, P., Leuenberger, H., Nyikos, P. 1970. *Helv. Phys. Acta* 43:39
 135. Nyikos, P., Gagneux, S., Huber, P., Kobel, H. R., Leuenberger, H. 1970. *Helv. Phys. Acta* 43:412
 136. Horen, D. J. 1971. *Nucl. Data B* 5:131
 137. Ball, J. B., Johns, M. W., Way, K. 1970. *Nucl. Data A* 8:407
 138. Geiger, J. S., Graham, R. L., Johns, M. W. 1969. *Can. J. Phys.* 47:949
 139. Cooper, J. A., Hollander, J. M., Rasmussen, J. O. 1967. *Nucl. Phys. A* 109:603
 140. Cooper, J. A., Hollander, J. M., Rasmussen, J. O. 1965. *Phys. Rev. Lett.* 15:680
 141. Holland, R. E., Lawson, R. D.,

- Lynch, F. J. 1971. *Ann. Phys. New York* 63:607
142. Weirauch, W., Schmidt-Ott, W.-D., Smend, F., Flammersfeld, A. 1968. *Z. Phys.* 209:289
143. Olin, A. 1970. *Phys. Rev. C* 1:1114
144. Smend, F., Borchert, I., Langhoff, H. 1971. *Z. Phys.* 248:326
145. Olin, A., Bainbridge, K. T. 1969. *Phys. Rev.* 179:450
146. Cooper, J. A. 1966. *Univ. Calif. Rep. UCRL-16910*
147. Lederer, C. M., Hollander, J. M., Perlman, I. 1967. *Table of Isotopes*. New York: Wiley. 6th ed.
148. Lacasse, W. M., Hamilton, J. H. 1971. *Nucl. Phys. A* 171:641
149. Byers, D. H., Stump, R. 1958. *Phys. Rev.* 112:77
150. Bainbridge, K. T. 1952. *Chem. Eng. News* 30:654; See also Ref. 152; *Phys. Rev.* 86:582
151. Mazaki, H., Nagatomo, T., Shimizu, S. 1972. *Phys. Rev. C* 5:1718
152. Porter, R. A., McMillan, W. G. 1960. *Phys. Rev.* 117:795
153. Leuenberger, H. et al 1970. *Helv. Phys. Acta* 43:411
154. Nishi, M., Shimizu, S. 1972. *Phys. Rev. B* 5:3218
155. Kostroun, V. O., Crasemann, B. 1968. *Phys. Rev.* 174:1535
156. Benczer-Koller, N., Fink, T. 1971. *Nucl. Phys. A* 161:123
157. Kistner, O. C., Jaccarino, V., Walker, L. R. 1962. *The Mössbauer Effect*, ed. D. M. J. Compton, A. H. Schoen, p. 264. New York: Wiley
158. Boyle, A. J. F., Bunbury, D. S. P., Edwards, C. 1962. *Proc. Phys. Soc.* 79:416
159. Bryukhanov, V. A., Delyagin, N. N., Opaljenke, A. A., Shpinel, V. S. 1962. *Zh. Eksp. Teor. Fiz.* 43:432
160. Gol'danskii, V. I., Makarov, E. F. 1965. *Phys. Lett.* 14:111
161. Bersuker, I. B., Gol'danskii, V. I., Makarov, E. F. 1965. *Zh. Eksp. Teor. Fiz.* 49:699
162. Gol'danskii, V. I., Makarov, E. F., Stukan, R. A. 1967. *J. Chem. Phys.* 47:4048
163. Lees, J. K., Flynn, P. A. 1965. *Phys. Lett.* 19:186
164. Lees, J. K., Flynn, P. A., 1968. *J. Chem. Phys.* 48:882
165. Ruby, S. L., Kalvius, G. M., Beard, G. B., Snyder, R. E. 1967. *Phys. Rev.* 159:239
166. Micklitz, H., Barrett, P. H. 1972. *Phys. Rev. B* 5:1704
167. Emery, G. T., Perlman, M. L. 1970. *Phys. Rev. B* 1:3885
168. Rothberg, G. M., Guimar, S., Benczer-Koller, N. 1970. *Phys. Rev. B* 1:136
169. Narcisi, R. S. 1959. *Harvard Univ. Dept. Phys. Tech. Rep.* 2-9
170. Geiger, J. S., Graham, R. L., Bergström, I., Brown, F. 1965. *Nucl. Phys.* 68:352
171. Marelus, A., Sparrman, P., Sundström, T. 1968. *Hyperfine Structure and Nuclear Radiations*, ed. E. Matthias, D. A. Shirley, p. 1043. New York: Wiley
172. Malliaris, A. C., Bainbridge, K. T. 1966. *Phys. Rev.* 149:958
173. Martin, R., Erickson, N. E., Perlman, M. L. 1969. Private communication, See Ref. 24
174. Makariunas, K., Kalinauskas, R., Davidonis, R. 1971. *Zh. Eksp. Teor. Fiz.* 60:1569
175. Ruby, S. L., Shenoy, G. K. 1969. *Phys. Rev.* 186:326
176. Carlson, T. A., Erman, P., Fransson, K. 1968. *Nucl. Phys. A* 111:371
177. Kankeleit, E., Boehm, F., Hager, R. 1964. *Phys. Rev. B* 134:747
178. Wagner, F. E. 1968. *Z. Phys.* 210:361
179. Turner, C. E., Jr., Hatch, E. N. 1972. *Bull. Am. Phys. Soc.* 17:559
180. Meggers, W. F. 1942. *Rev. Mod. Phys.* 14:96
181. Dieke, G. H. 1968. *Spectra and Energy Levels of Rare Earth Ions in Crystals*. New York: Interscience
182. Schaller, H., Kaindl, G., Wagner, F., Kienle, P. 1967. *Phys. Lett. B* 24:397
183. Hopke, P. K., Naumann, R. A. 1969. *Phys. Rev.* 185:1565
184. Johansson, A. et al 1967. *Phys. Lett. B* 26:83
185. Svahn, B., Johansson, A., Nyman, B., Malmsten, G., Pettersson, H. 1968. *Z. Phys.* 210:466
186. Marelus, A. 1968. *Ark. Fys.* 37:427
187. Asaro, F., Perlman, I. 1957. *Phys. Rev.* 107:318
188. Huizenga, J. R., Rao, C. L., Engelkemeir, D. W. 1957. *Phys. Rev.* 107:319
189. Artna-Cohen, A. 1971. *Nucl. Data B* 6:287
190. Nève de Mévergnies, M. 1970. *Phys. Lett. B* 32:482
191. Freedman, M. S., Porter, F. T., Wagner, F., Jr., Day, P. P. 1957. *Phys. Rev.* 108:836
192. Michel, M. C., Asaro, F., Perlman, I. 1957. *Bull. Am. Phys. Soc.* 2:394

193. Mazaki, H., Shimizu, S. 1966. *Phys. Lett.* 23:137, 491
194. Mazaki, H., Shimizu, S. 1966. *Bull. Inst. Chem. Res. Kyoto* 44:394
195. Schuurmans, P. 1946. *Physica The Hague* 11:419
196. Kiess, C. C., Humphreys, C. J., Laun, D. D. 1946. *J. Res. Nat. Bur. Stand. A* 37:57
197. Bearden, J. A., Burr, A. F. 1967. *Rev. Mod. Phys.* 39:125
198. Shimizu, S., Mazaki, H. 1965. *Phys. Lett.* 17:275
199. Mazaki, H., Shimizu, S. 1966. *Phys. Rev.* 148:1161
200. Nève de Mévergnies, M. 1968. *Phys. Lett. B* 26:615
201. Nève de Mévergnies, M. 1969. *Phys. Rev. Lett.* 23:422
202. Nève de Mévergnies, M. 1971. Private communication
203. Nève de Mévergnies, M. 1972. Private communication
204. Novakov, T., Hollander, J. M. 1964. *Phys. Lett.* 13:301
205. Novakov, T., Janičević, P. 1967. *Z. Phys.* 205:359
206. Novakov, T., Hollander, J. M. 1968. *Phys. Rev. Lett.* 21:1133
207. Novakov, T., Stepić, R., Janičević, P. 1969. *Fizika Suppl.* 1:53
208. Novakov, T., Hollander, J. M. 1969. *Bull. Am. Phys. Soc.* 14:524
209. Martin, B., Schulé, R. 1972. *Proc. Int. Conf. on Inner Shell Ionization Phenomena*. Amsterdam: North-Holland
210. Kemeny, P. 1968. *Proc. Conf. Electron Capture and Higher-Order Processes in Nuclear Decays*, p. 342. Budapest: Eötvös Lóránd Phys. Soc.
211. Verheul, H. 1967. *Nucl. Data B* 2(3): 65
- 211a. Johnson, J. A., Harbottle, G. 1972. Private communication
212. Bergamini, P. G., Palmas, G., Piantelli, F., Rigato, M. 1967. *Phys. Rev. Lett.* 18:468
213. Kemeny, P. 1968. *Rev. Roum. Phys.* 13:485
214. Zoller, W. H., Hopke, P. K., Fashing, J. L., Macias, E. S., Walters, W. B. 1971. *Phys. Rev. C* 3:1699
215. Graeffe, G., Walters, W. B. 1967. *Phys. Rev.* 153:1321
216. Alder, K., Hadermann, J., Raff, U. 1969. *Phys. Lett. A* 30:487
217. Crawford, M. F., Schawlow, A. L. 1949. *Phys. Rev.* 76:1310
218. Tucker, T. C., Roberts, L. D., Nestor, C. W., Jr., Carlson, T. A., Malik, F. B. 1969. *Phys. Rev.* 178:998
219. Fricke, B., Waber, J. T. 1972. *Phys. Rev. B* 5:3445
220. Lamb, W. E. 1941. *Phys. Rev.* 60:817
221. Sternheimer, R. 1950. *Phys. Rev.* 80:102
222. *Ibid* 1951. 84:244
223. *Ibid* 1952. 86:316
224. Ingalls, R. 1967. *Phys. Rev.* 155:157
225. Ingalls, R., Drickamer, H. G., De Pasquali, G. 1967. *Phys. Rev.* 155:165
226. Moyzis, J. A., Jr., Drickamer, H. G. 1968. *Phys. Rev.* 171:389
227. Snyder, N. S. 1969. *Phys. Rev.* 178:537
228. Akhmetova, B. G., Plets, Yu., M., Tulinov, A. F. 1969. *Zh. Eksp. Teor. Fiz.* 56:813; 1969. *Sov. Phys. JETP* 29:442
229. Fraser, B. C., Danner, H., Pepinsky, R. 1955. *Phys. Rev.* 100:745
230. Gemmell, D. S., Mikkelsen, R. C. 1972. *Phys. Rev. B* 6:1613
231. Schiff, L. I. 1963. *Phys. Rev.* 132:2194
232. Pound, R. V., Rebka, G. A., Jr. 1960. *Phys. Rev. Lett.* 4:274
233. Josephson, B. D. 1960. *Phys. Rev. Lett.* 4:341
234. Bahcall, J. N. 1964. *Astrophys. J.* 139:318
235. Iben, I., Jr., Kalata, K., Schwartz, J. 1967. *Astrophys. J.* 150:1001
236. Schatzman, E. 1958. *White Dwarfs*, p. 143. Amsterdam: North-Holland
237. Valadres, M., Walen, R. J., Briancon, C. 1966. *C. R. Acad. Sci. B* 263:213
238. Gelletly, W., Geiger, J. S., Merritt, J. S. 1970. *Can. J. Phys.* 48:993
- 238a. Walen, R. J., Valadres, M., Briancon, C. 1971. *J. Phys. Suppl. C* 32:4-145
239. Sliv, L. A. 1953. *Zh. Eksp. Teor. Fiz.* 25:7
240. Lombard, R., Rys, F. 1962. *Nucl. Phys.* 31:163
241. Perdrisat, C. F., Brunner, J. H., Leisi, H. J. 1962. *Helv. Phys. Acta* 35:175
242. Wiener, R., Chasman, C., Harihar, P., Wu, C. S. 1963. *Phys. Rev.* 130:1069
243. Frauenfelder, H., Steffen, R. M. 1965. *Alpha-, Beta-, and Gamma-Ray Spectroscopy*, ed. K. Siegbahn, p. 1182-88. Amsterdam: North-Holland
244. Alder, K., Baur, G., Raff, U. 1971. *Phys. Lett. A* 34:163

245. Carlson, T. A., Lu, C. C., Tucker, T. C., Nestor, C. W., Malik, F. B. 1970. *Oak Ridge Nat. Lab. Rep. ORNL-4614*
- 245a. Rubinson, W., Perlman, M. L. 1972. *Phys. Lett. B* 40:352
246. Durand, L., III. 1964. *Phys. Rev. B* 135:310
247. Wilkinson, D. H. 1970. *Nucl. Phys. A* 150:478
248. Alder, K., Baur, G., Raff, U. 1971. *Helv. Phys. Acta* 44:514
249. Bergkvist, K.-E. 1971. *Physica Scripta* 4:23
250. Brodzinski, R. L., Conway, D. C. 1965. *Phys. Rev. B* 138:1368
251. Huster, E., Verbeek, H. 1967. *Z. Phys.* 203:435
252. Ewbank, W. B. 1966. *Nucl. Data B* 1(2):23
253. Krutov, V. A., Fomenko, V. N. 1968. *Ann. Phys. Leipzig* 21:291
254. Krutov, V. A., Fomenko, V. N. 1969. *Izv. Akad. Nauk SSSR Ser. Fiz.* 33:84 (*Bull. Acad. Sci. USSR Phys. Ser.* 33:79)
255. Krutov, V. A., Knyazkov, O. M. 1970. *Ann. Phys. Leipzig* 25:10
256. Hannon, J. P., Trammell, G. T. 1968. *Phys. Rev. Lett.* 21:726
257. Henley, E. M. 1969. *Ann. Rev. Nucl. Sci.* 19:367
258. Emery, G. T., Perlman, M. L. 1966. *Phys. Rev.* 151:984, 161:1294
259. Pauli, H.-C., Alder, K. 1967. *Z. Phys.* 202:255
260. Hager, R. S., Seltzer, E. C. 1969. *Nucl. Data A* 6:1
261. Dirac, P. A. M. 1937. *Nature* 139:323
262. Dirac, P. A. M. 1938. *Proc. Roy. Soc. London A* 165:198
263. Gamow, G. 1967. *Phys. Rev. Lett.* 19:759
264. Wilkinson, D. H. 1958. *Phil. Mag.* 3:582
265. Dyson, F. J. 1967. *Phys. Rev. Lett.* 19:1291
266. Spector, R. M. 1972. *Phys. Rev. A* 5:1323
267. Konarski, J. M., Wszolek, B., Kukiel, E. 1969. *Phys. Lett. A* 30:529
268. Wszolek, B., Kinarski, M., Kukiel, E. 1967. *Acta Phys. Pol.* 32:323
269. Ibid 1969. 35:859
270. Ibid 1970. *Phys. Lett. A* 31:37
271. Anderson, J. L., Spangler, C. W. 1971. *Bull. Am. Phys. Soc.* 16:1180
272. Shinohara, T., Fujioka, M. 1972. Private communication
273. Watson, R. E., Missetich, A. A., Hodges, L. 1971. *J. Phys. Chem. Solids* 32:709
274. Emery, J. F., Reynolds, S. A., Wyatt, E. I., Gleason, G. I. 1972. *Nucl. Sci. Eng.* 48:319

CONTENTS

COLLIDING-BEAM ACCELERATORS, <i>C. Pellegrini</i>	1
ISOSPIN IMPURITIES IN NUCLEI, <i>George F. Bertsch, Aram Mekjian</i>	25
CALCULATION OF FISSION BARRIERS FOR HEAVY AND SUPERHEAVY NUCLEI, <i>James Rayford Nix</i>	65
ELECTROMAGNETIC TRANSITIONS AND MOMENTS IN NUCLEI, <i>Shiro Yoshida, Larry Zamick</i>	121
PERTURBATION OF NUCLEAR DECAY RATES, <i>G. T. Emery</i>	165
DEEP INELASTIC ELECTRON SCATTERING, <i>Jerome I. Friedman, Henry W. Kendall</i>	203
EVIDENCE FOR REGGE POLES AND HADRON COLLISION PHENOMENA AT HIGH ENERGIES, <i>Charles B. Chiu</i>	255
THERMAL BREEDER REACTORS, <i>Alfred M. Perry, Alvin M. Weinberg</i>	317
RADIATION DAMAGE MECHANISMS AS REVEALED THROUGH ELECTRON SPIN RESONANCE SPECTROSCOPY, <i>Harold C. Box</i>	355
NUCLEAR APPLICATIONS IN ART AND ARCHAEOLOGY, <i>I. Perlman, F. Asaro, H. V. Michel</i>	383
NUCLEAR LEVEL DENSITIES, <i>J. R. Huizenga, L. G. Moretto</i>	427
THE NUCLEON-NUCLEON EFFECTIVE RANGE EXPANSION PARAMETERS, <i>H. P. Noyes</i>	465
SOME RELATED ARTICLES APPEARING IN OTHER <i>Annual Reviews</i>	485
AUTHOR INDEX	487
CUMULATIVE INDEX OF CONTRIBUTING AUTHORS, VOLUMES 13 TO 22	500
CUMULATIVE INDEX OF CHAPTER TITLES, VOLUMES 13 TO 22	501